Lithospheric folding in Iberia

S. Cloetingh,[1] E. Burov,[2] F. Beekman,[1] B. Andeweg,[1] P. A. M. Andriessen,[1]
D. Garcia-Castellanos,[1] G. de Vicente,[3] and R. Vegas[3]

Received 31 July 2001; revised 27 December 2001; accepted 15 January 2002; published 4 October 2002.

[1] Integration of stress indicator data, gravity data, crustal kinematics data, and analysis of topography and recent vertical motions demonstrates the occurrence of consistently oriented spatial patterns of large-scale Alpine to recent intraplate deformation in Iberia. The inferred upper crustal and lithospheric deformation patterns and the timing of the associated expressions at or near the surface support the existence of a close coupling with plate boundary processes operating at the margins of Iberia. Patterns of lithosphere and upper crustal folds are oriented perpendicular to the main axis of present-day intraplate compression in Iberia inferred from structural analysis of stress indicator data and focal mechanism solutions. These findings suggest the presence of lithospheric folds, with wavelengths compatible with theoretical predictions of folding wavelengths of Variscan lithosphere. Stress-induced intraplate deformation set up by plate interactions is compatible with indications for the absence of present-day deep mantle-lithosphere interactions inferred from seismic tomography. *INDEX TERMS:* 8105 Tectonophysics: Continental margins and sedimentary basins; 8107 Tectonophysics: Continental neotectonics; 8122 Tectonophysics: Dynamics, gravity and tectonics; 8159 Tectonophysics: Rheology—crust and lithosphere; 8164 Tectonophysics: Stresses—crust and lithosphere; *KEYWORDS:* lithospheric folding, intraplate deformation, Iberia, recent vertical motions, drainage patterns.
Citation: Cloetingh, S., E. Burov, F. Beekman, B. Andeweg, P. A. M. Andriessen, D. Garcia-Castellanos, G. de Vicente, and R. Vegas, Lithospheric folding in Iberia, *Tectonics*, *21*(5), 1041, doi:10.1029/2001TC901031, 2002.

1. Introduction

[2] The nature of intraplate stress fields in continental lithosphere and its relationship to plate tectonic driving forces has been subject to a large number of observational [e.g., *Zoback*, 1992; *Van der Pluim et al.*, 1997] and modeling studies [e.g., *Richardson et al.*, 1979; *Cloetingh and Wortel*, 1985; *Bada et al.*, 1998; *Golke and Coblentz*, 1996]. These studies have revealed the existence of consistently oriented first-order patterns of intraplate stress in for example the Northwestern European platform and the North American craton. The effect of these stresses on vertical motions in the lithosphere expressed in terms of, for example, apparent sea level fluctuations [*Cloetingh et al.*, 1985], foreland bulges [*Ziegler et al.*, 2002], basin inversion [*Ziegler et al.*, 1995, 1998], and lithosphere folding [*Martinod and Davy*, 1994; *Cloetingh et al.*, 1999] has been demonstrated to be an important element in the dynamics of intraplate continental interiors [*Cloetingh*, 1988; *Van der Pluim et al.*, 1997; *Marshak et al.*, 1999]. In particular, the role of continental lithosphere folding appears to be more important in the large-scale deformation of continental lithosphere than till hitherto thought [*Cloetingh et al.*, 1999; *Caporali*, 2000]. The large wavelength of the associated vertical motions implies the need for an integration of the available data for relatively large areas [*Ben-Avraham and Ginzburg*, 1990], often in excess of the size of the domains of regional structural and geophysical studies targeting on specific substructural provinces. The recent documentation of lithospheric folding in Variscan lithosphere in Brittany [*Bonnet et al.*, 2000] as well as in the adjacent Paris Basin [*Lefort and Agarwal*, 1996; *Guillocheau*, 2002] raises the question whether lithosphere folding could also play a key role in affecting recent vertical motions within micro plates with a Variscan structural grain close to and overprinted by recent plate boundary activity. As known, lithosphere folding is a very effective mechanism for propagation of tectonic deformation far from the active plate boundaries [e.g., *Stephenson and Cloetingh*, 1991; *Burov et al.*, 1993; *Ziegler et al.*, 1995; *Burov and Molnar*, 1998]. It is thus probably the only mechanism not implying active mantle processes that could allow for a plausible explanation of active deformation in the central parts of Iberia.

[3] In this paper we integrate new data on the Iberian stress field and the record of recent vertical motions. We demonstrate through numerical modeling that lithosphere folding could be a major contributor to the current anomalous topography of the Iberian continent. The focus of the present paper is on the Late Neogene - recent intraplate deformation of Iberia. As pointed out recently by several authors [*Vegas et al.*, 1990; *Van Wees et al.*, 1996; *Andeweg*, 2002], large-scale intraplate deformation of Iberia has also occurred from Early Tertiary onward. In the eastern part of the Iberian Peninsula the structural grain of the mechanical coupling with the Pyrenean orogeny is still recognizable with indication for small-scale lithosphere folding [*Verges et al.*, 1998; *Waltham et al.*, 2000].

[4] The subsequent superposition of the intraplate deformation induced by the Betic orogeny (see Figure 1) has

[1]Faculty of Earth and Life Sciences, Vrije Universiteit Amsterdam, The Netherlands.
[2]Laboratoire de Tectonique, University of P. et M. Curie, Paris, France.
[3]Faculty of Geological Sciences, Universidad Complutense Madrid, Spain.

0278-7407/02/2001TC901031$12.00

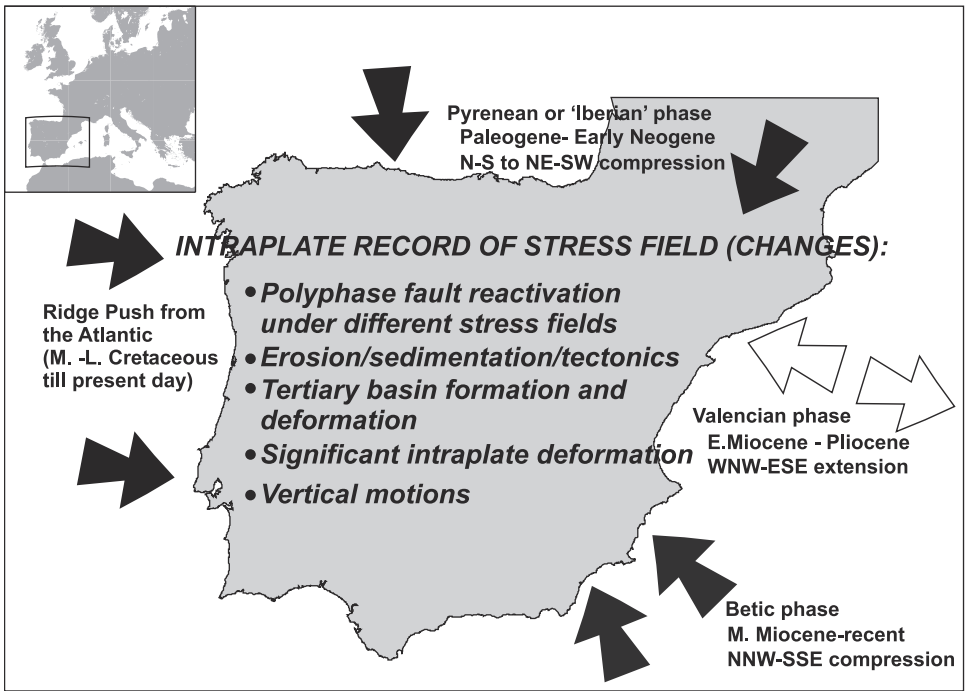

Figure 1. Plate tectonic setting and timing of Alpine to recent plate boundary reorganizations and their impact on intraplate deformation of Iberia and related processes in basin (de)formation in Iberia, the Atlantic and western Mediterranean region adjacent to Iberia.

resulted in a complex interference pattern of deformation in the northeastern segment of Iberia being resolved by current field studies [*Andeweg*, 2002] and geothermochronology [*Juez Larre and Andriessen*, 2002]. More constraints are needed on this area to model the interference patterns. As in the central and western part of Iberia the relation between the Betic orogeny and induced intraplate deformation is more straightforward, this area forms the focus of our recent modeling effort.

[5] This succession of polyphase deformation is an important factor in understanding the Late Neogene to present-day record of intraplate deformation. We have incorporated the large-scale effects of Early Tertiary tectonics in the lithospheric configuration adopted in the modeling of the response of Iberia to recent plate reorganizations.

2. Iberia: Record of Intraplate Deformation in the Absence of Mantle Dynamics?

[6] Recent studies are providing accumulating evidence for a strong impact of crustal kinematics on the record of vertical motions of the Iberian Peninsula [e.g., *Friend and Dabrio*, 1996; *Casas-Sainz et al.*, 2000]. The location of the Iberian Peninsula at close proximity to (recently) active plate boundaries at its southern and western margins [e.g., *Roest and Srivastava*, 1991; *Van Wees et al.*, 1992], the Pyrenean orogen [*Munoz*, 1992; *Verges et al.*, 1998; *Millan et al.*, 1995] at the north as well as active Late Neogene extensional basin formation at its eastern margin [e.g., *Janssen et al.*, 1993; *Docherty and Banda*, 1995] makes it an almost ideal natural laboratory for the analysis of the underlying lithospheric controls. A clear sequence in time and space can be recognized for the main events along the boundaries of Iberia (Figure 1). Plate reorganization at the northern boundary was initiated at late Cretaceous time and lasted till approximately 24 Ma [*Roest and Srivastava*, 1991], whereas the convergent plate boundary interaction culminating in the Betics orogeny essentially took place from Late Oligocene times onward. Reactivation of the Atlantic ocean-continent boundary on the Western Iberian margin has been documented for Late Miocene times [*Masson et al.*, 1994]. Simultaneously, Miocene deformation took place in the Mesozoic Lusitanian Basin [*Ribeiro et al.*, 1990]. The basins of central Spain were reactivated multiple times since the Paleogene [*Vegas and Banda*, 1982; *Vegas et al.*, 1990; *Van Wees et al.*, 1996; *De Bruijne and Andriessen*, 2000, 2002], suggesting a major control by the onset of the Pyrenean and Betic orogenies (Figure 1). Major border fault activity occurred from Middle Miocene time onward in the Madrid Basin, leading to local creation of pop-up structures.

[7] Seismic tomography data of the western Mediterranean [*Wortel and Spakman*, 2000] provide evidence for a major Neogene retreat of plate subduction in an eastward direction, essentially leaving the main part of the Iberian Peninsula absent to intensive deep mantle-lithosphere interaction with a remnant of deep seismicity only restricted to the southeastern margin of Iberia [*Blanco and Spakman*, 1993]. At first sight this appears incompatible with the widespread occurrence of intraplate deformation continuing up to present day.

[8] Figure 2 displays the main structural features and the spatial pattern of recent vertical motions in Iberia. The

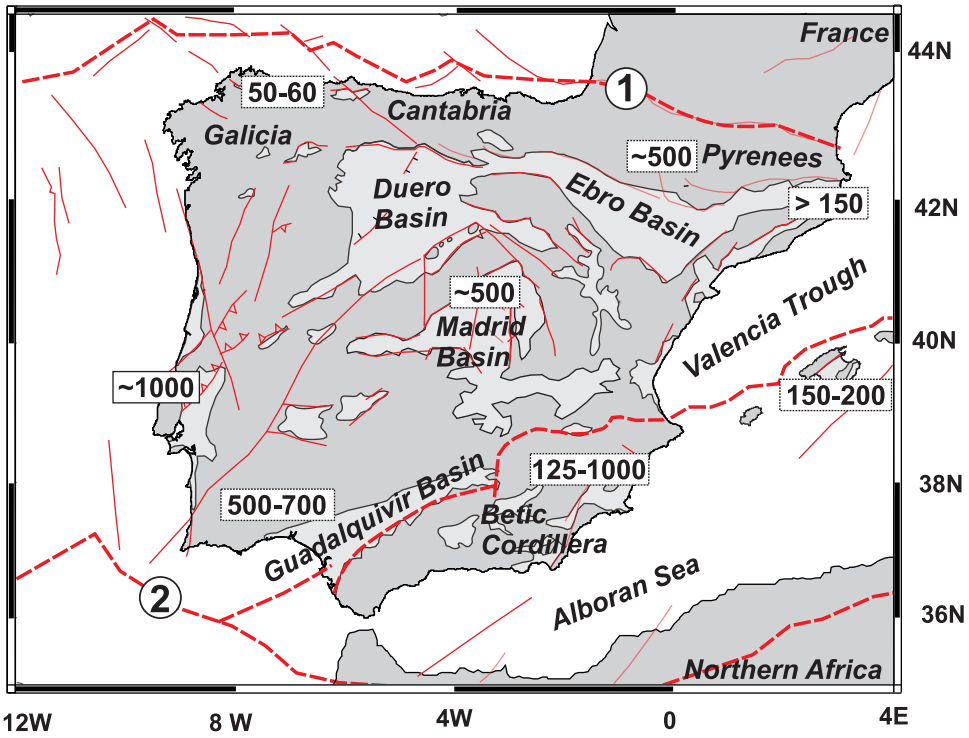

Figure 2. Main structural features of Iberia, northern (1) and southern (2) plate margins, and patterns of anomalous recent uplift. Timing of phases after *Roest and Srivastava* [1991], *Masson et al.* [1994], *De Jong et al.* [1992], *Ribeiro et al.* [1990], *de Vicente et al.* [1996], *Janssen et al.* [1993], and *Andeweg* [2002]. Numbers in boxes refer to quantitative estimates of the magnitude (in meters) of the Pliocene-Quaternary uplift recorded in Iberia [*Janssen et al.*, 1993; *Zeck et al.*, 1992; *Andeweg*, 2002].

mechanisms underlying these observed vertical motions are not fully resolved, but processes of slab detachment and or lithospheric delamination appear to play a minor role [*Janssen et al.*, 1993; *Docherty and Banda*, 1995; *Seber et al.*, 1996]. The presently available geophysical data for upper mantle structure and seismicity [*Blanco and Spakman*, 1993; *Seber et al.*, 1996] point also strongly in this direction. At the same time, rift shoulder uplift of the eastern margin of Iberia, induced by the Late Neogene extension in the Valencia Trough [*Janssen et al.*, 1993] and the Alboran Sea [*Docherty and Banda*, 1995; *Cloetingh et al.*, 1992], has occurred.

[9] A first-order question is whether the above mantle processes are overprinted by a contribution from intralithospheric mechanisms. Below we demonstrate that recent evidence on the stress field and the gravity data of Iberia support an important role of continental lithosphere folding in the Late Cenozoic to recent tectonic evolution.

3. Constraints on Vertical Motions

[10] Following the advent of quantitative subsidence analysis, a large number of studies have addressed the record of vertical motions of different basins in the Iberian continent. Most of these studies have been focusing on either the Mesozoic record of central Atlantic breakup within areas such as the Iberian Chain [*Van Wees et al.*, 1998; *Casas and Salas*, 1993], the Lusitanian Basin [*Stapel et al.*, 1996] or the pre-Betic [*Peper and Cloetingh*, 1992] or on the marine stages of flexural basins related to Alpine thrust belt emplacement in the Betic foreland [*Van der Beek and Cloetingh*, 1992; *Garcia-Castellanos et al.*, 2002] and the Ebro Basin [*Gaspar-Escribano et al.*, 2001]. Oligocene and Miocene deformation left a major imprint in the eastern margin of Iberia, at first sight not affecting the Variscan core of the peninsula. Compared to the large amount of work focusing on the earlier record, the attention paid so far on the tectonic controls of more recent vertical motions have been relatively minor. Backstripping analysis and forward modeling of the record of the Neogene pull-apart basins of eastern Iberia (Figure 3a) has, however, revealed the existence of a large Pliocene-Quaternary uplift of a typical magnitude of 500 m over a large part of Iberia [*Cloetingh et al.*, 1992; *Janssen et al.*, 1993; *Docherty and Banda*, 1995]. Quaternary uplift in the Betic foreland can be quantified by Late Miocene marine sediments that are elevated to more than 1200 m in several sierras, related to the continuous convergence between the African and Eurasian plates [*Andeweg and Cloetingh*, 2001]. Similarly, fission track studies have been able to assess the record of differential vertical motions for a number of areas in the Iberian Peninsula, including the Betics [*Zeck et al.*, 1992], the southeastern margin of Iberia [*Stapel*, 1999], the

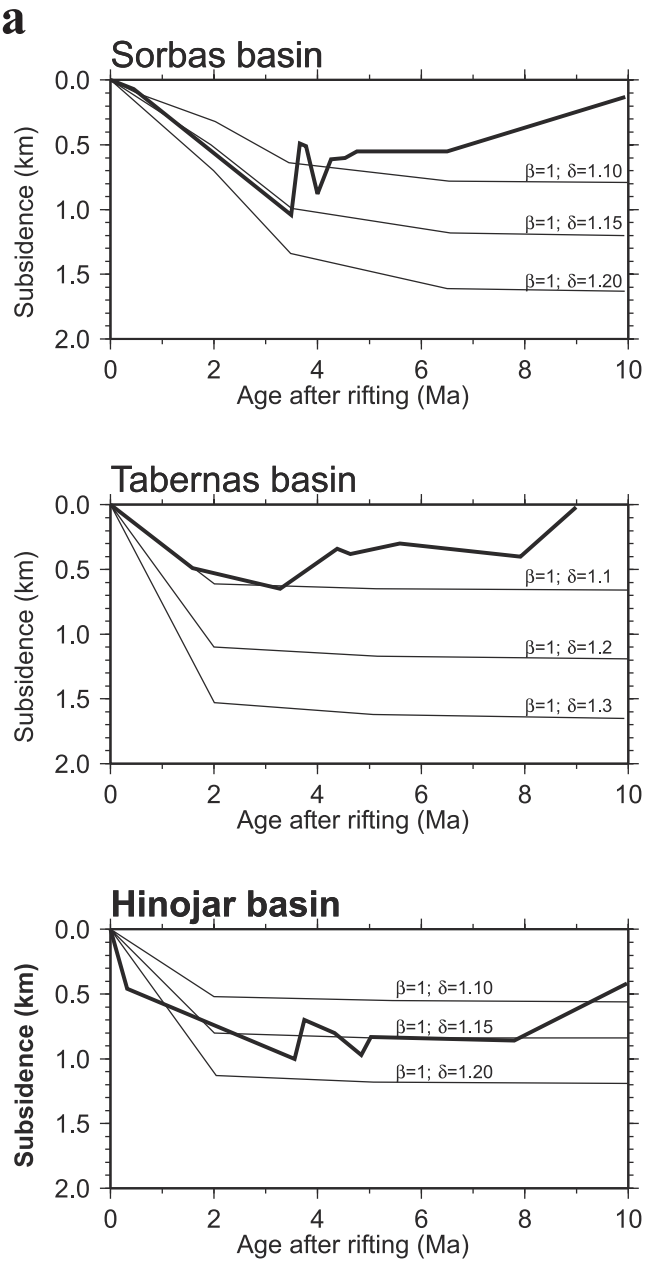

Western margin of Iberia [*Stapel*, 1999], the Pyrenees [*Fitzgerald et al.*, 1999] and the Spanish Central System [*De Bruijne and Andriessen*, 2000, 2002]. These studies have revealed a long and complex record of polyphase deformation of Iberia with a concentration of major rift-related early Mesozoic thermal rejuvenation concentrated at the western and eastern margins of Iberia. Apatite fission track studies [*Stapel*, 1999; *De Bruijne and Andriessen*, 2000, 2002] have also demonstrated a simultaneously occurring rapid post-Miocene cooling phase concentrated in structural highs in both the western margin of Iberia as well as the Spanish Central System (SCS) (Figures 3b and 3c).

[11] In the central part of Iberia the topography was around sea level in Late Cretaceous time, prior to the onset of north-south oriented compressional stress from the Pyrenean collision, which was leading to local deformation in the area, accompanied by a first phase of accelerated cooling around Late Eocene to Early Oligocene times (around 36 Ma). This was followed by a phase of significant accelerated cooling in central Spain around Middle Miocene times (15 Ma), followed by a very pronounced phase of accelerated cooling from Early Pliocene (5 Ma) onward [*De Bruijne and Andriessen*, 2000] (also see Figure 3b). The largest amount of cooling occurred in the Sierra de Guadarrama (eastern SCS) during the Pliocene (Figure 3b), and has been shown to be the result of a major phase of up to 6 km Pliocene uplift accompanied by erosion [*De Bruijne and Andriessen*, 2000; *de Bruijne and Andriessen*, 2002]. These authors relate this to the far-field effect of the ongoing Betic compression. Most denudation in the Sierra de Gredos (western SCS) occurred from the Middle Eocene to the Lower Miocene and can be related to a N-S stress field induced by the Pyrenean compression. The difference in trend of the preexisting lineaments (E-W for Gredos; NE-SW for Guadarrama) explains the difference in the relative importance of these far-field stresses on vertical motions in the area [*De Bruijne and Andriessen*, 2002]. This idea is supported by a combined study of structural elements and sedimentary sequences along the border between the NE-SCS and the Madrid Basin [*Andeweg*, 2002].

[12] Thermal modeling of the fission track data supports a scenario of enhanced simultaneous uplift and erosion from Pliocene to present day, providing independent support for

Figure 3. (opposite) Constraints on timing and magnitude of Late Neogene vertical motions from quantitative subsidence analysis and fission track analysis [after *Cloetingh et al.*, 1992; *Stapel*, 1999; *De Bruijne and Andriessen*, 2002]. See Figure 5a for locations of mentioned sample sites. (a) Subsidence curves, demonstrating recent uplift. Tectonic subsidence (solid lines) reconstructed for three late Neogene pull-apart basins in the internal zone of the Betic Cordilleras (SE Spain). Fine lines are theoretical subsidence curves calculated for differential stretching in crust ($\delta \neq 1$) and in the absence of mantle stretching ($\beta = 1$). Note that all basins demonstrate acceleration in late stage uplift strikingly deviating from a prediction of thermal models of basin subsidence. (b) Fission track ages and length distributions and thermal histories giving the best fit to these data, for 5 rock samples from the Spanish Central System (SCS). Thermal histories are obtained with the Monte Trax program [*Gallagher*, 1995], and are shown as black lines within the 100 best fit envelopes (gray shaded). The modeled track length distributions are projected on the measured track length distribution [from *De Bruijne and Andriessen*, 2000, 2002]. (c) Same as Figure 3b, but now for rock samples for western Iberia (Lusitanian Basin (LB) and Serra da Estrela (SE)) and for southern-western Iberia (Sierra Morena (SM)). Plotted are a range of cooling histories that fit the fission track age and track length distribution. Also shown are Monte Carlo boxes based on the information from the fission track data and geologic observations. The gray-shaded area is the partial annealing zone (PAZ) [from *Stapel*, 1999].

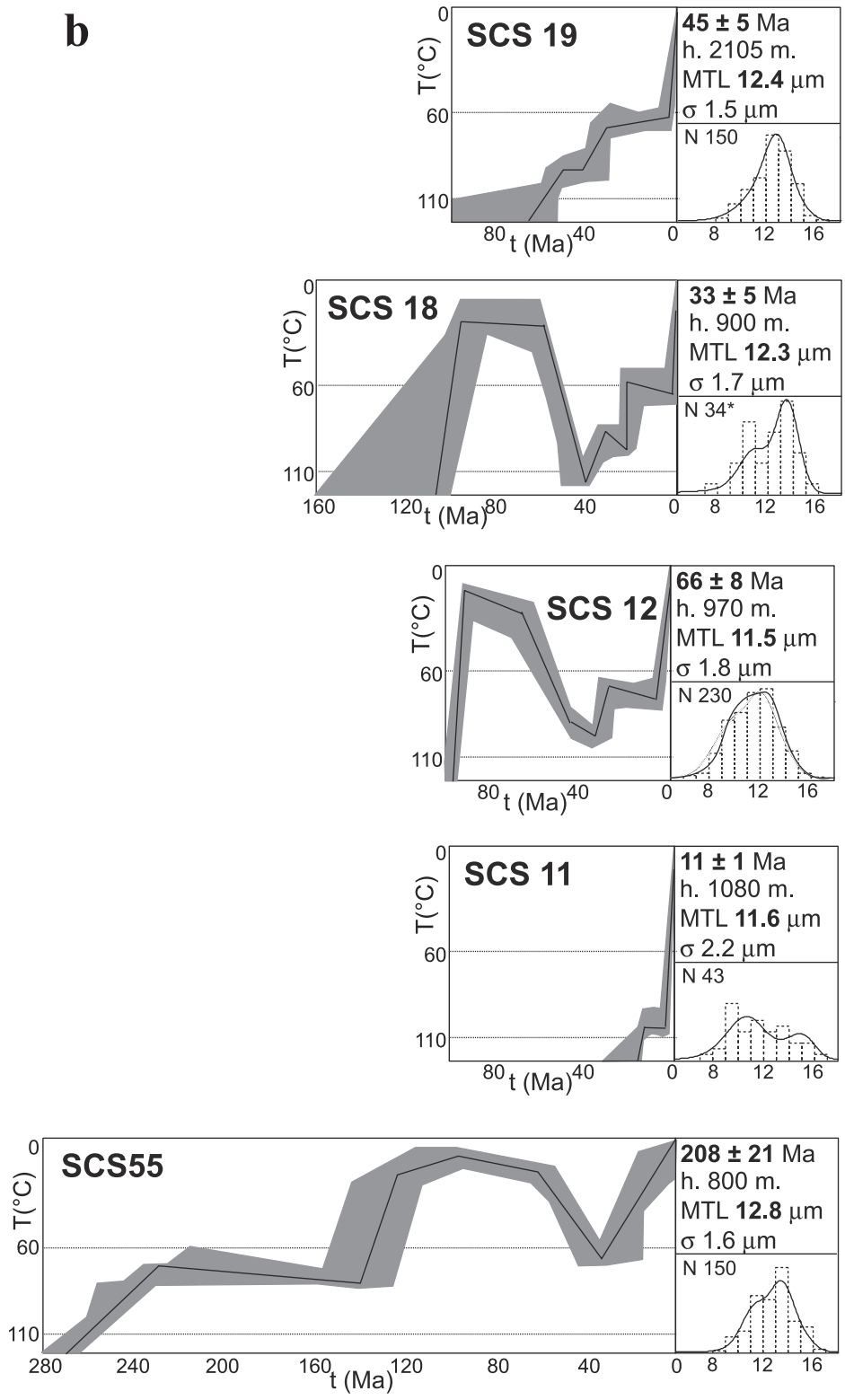

Figure 3. (continued)

an ongoing Betic compression [*de Bruijne and Andriessen*, 2002]. Other scenarios, including a mid-Miocene uplift phase creating a mountain range eroded during Pliocene due to a change of drainage pattern, are incompatible with the observed accelerated cooling in the area during the Pliocene and Quaternary [*de Bruijne and Andriessen*, 2002].

[13] Recent data from geodetic leveling and VLBI laser ranging [*Rutigliano et al.*, 2000] point to current vertical

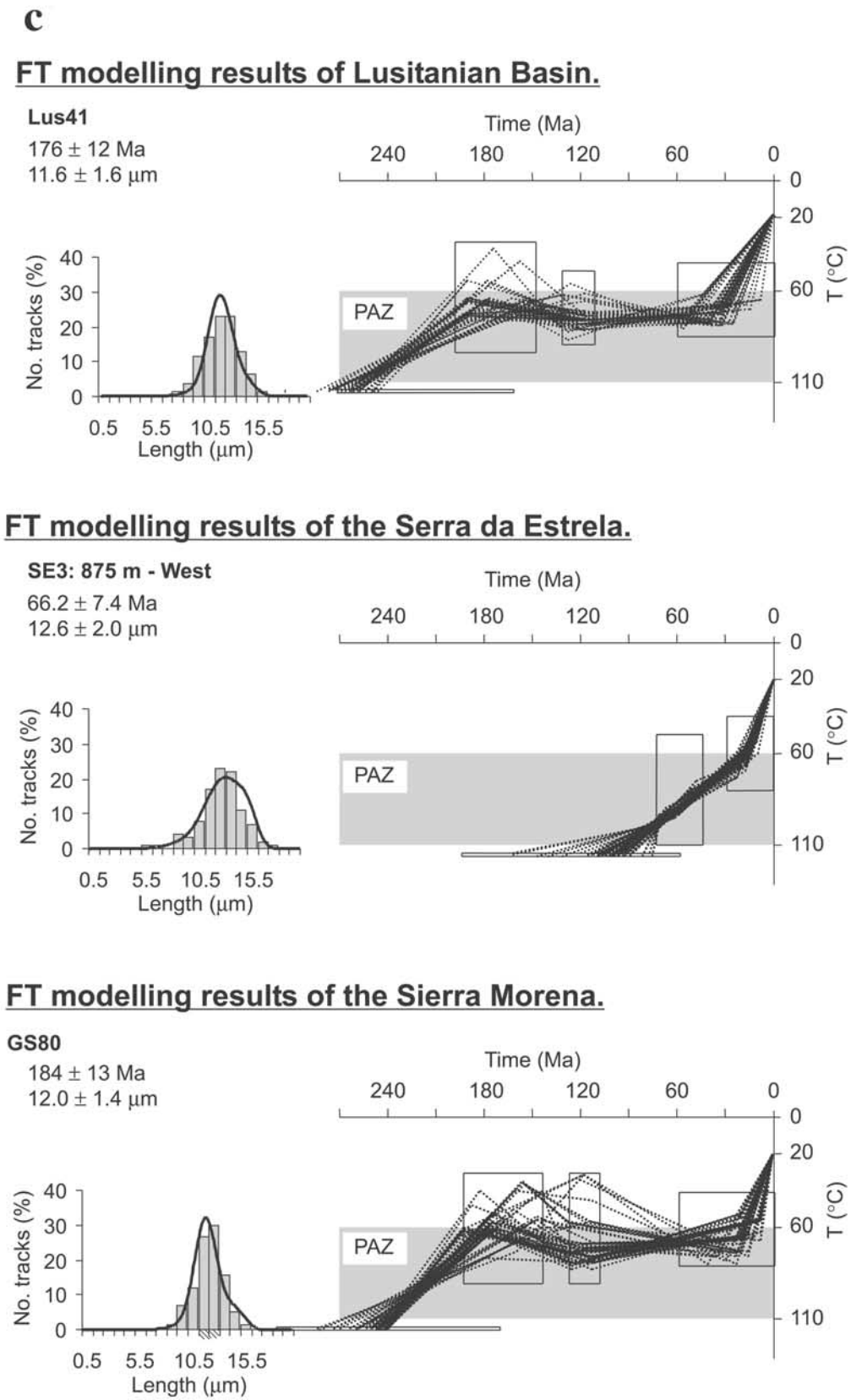

Figure 3. (continued)

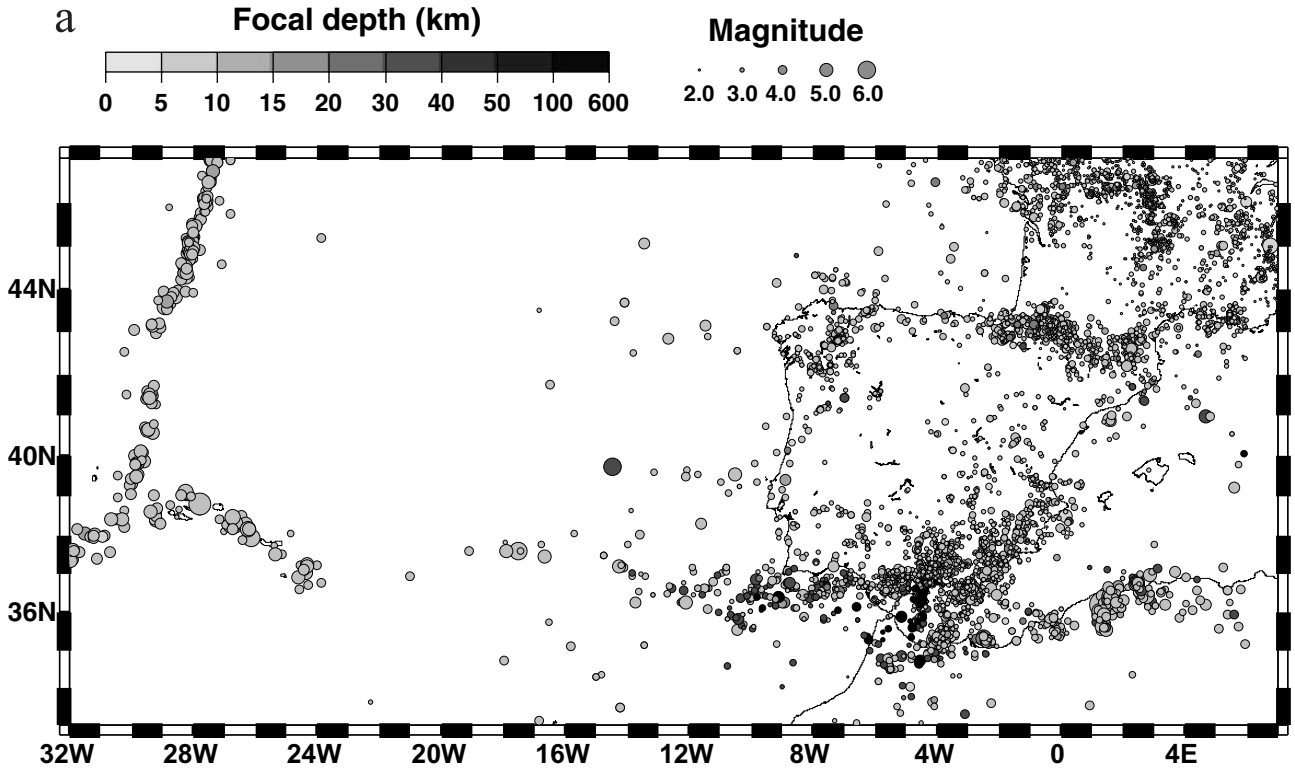

Figure 4. Present-day deformation indicated by intraplate seismicity and stress field indicator data. (a) Distribution of seismicity in Iberia from 1980 to 1998. Mb magnitudes, compilation of on-line available data of Instituto Geografica Nacional of Spain (IGN) and Northern California Earthquake Data Center (NCEDC)/Council of the National Seismic System (CNSS) [*Andeweg et al.*, 1999]. Note that seismicity is not restricted to the plate boundaries only (see Figure 2), with a relatively high level of seismic activity in continental lithosphere. (b) Present-day stress trajectories (thin blue lines) in Iberia and the western Mediterranean based on fault slip data, borehole breakout data and focal mechanism solutions (all denoted by the black and white arrows) [after *Andeweg*, 2002]. Thin red lines denote the major tectonic structures and lineaments. The spatial orientation (''fanning'') of the first-order patterns in the present-day stress regime suggest a strong control by plate boundary processes (collision Africa/Eurasia, ridge push from the Atlantic) and large-scale weakness zones, such as former active plate boundaries (Pyrenees).

uplift of the Spanish Central System of the order of 1 mm/yr. The above findings suggest that a long-lasting and still active tectonic control is affecting the topography of Iberia. The first indications from GPS networks in the Iberian Peninsula [*Fernandes et al.*, 2000; *Castellote et al.*, 2000] are pointing to consistently oriented horizontal motions, pointing to the question whether these recent vertical motions are a byproduct of continuing crustal shortening in the peninsula [*Andeweg and Cloetingh*, 2001], amplifying preexisting differential topography.

[14] In line with the focus of this paper on large-scale intraplate deformation we refrain from a detailed discussion of structural features on field scale and spatial dimensions at kilometer scale not addressed by the modeling.

[15] In this context it should be noted that the focus of this paper is on the far-field effects of the Betic collision on intraplate deformation and stress propagation in the Iberian micro continent. In this context we explicitly do not address the internal structuring of the Betic system itself (see, e.g., *Ziegler et al.* [1998, 2002] for a general discussion of the fine structure of the mechanical coupling between orogen and foreland lithosphere).

4. Stress Indicator Data and Present-Day Stress Regime of Iberia

[16] Being close to active plate boundaries, the southern margin of Iberia is characterized by a high level of seismicity. The seismicity, however, is not restricted to this area (see Figure 4a) as manifested by a high level of neotectonics in the western margin of Iberia, including the Tajo Valley and the Galicia margin. The same can be said about the central part of Iberia, with significant seismicity detected in the Madrid basin. Therefore it appears that the seismicity, which is concentrated along preexisting structural weakness zones, exhibits a typical intraplate type of lithosphere deformation. A large number of focal mechanism studies

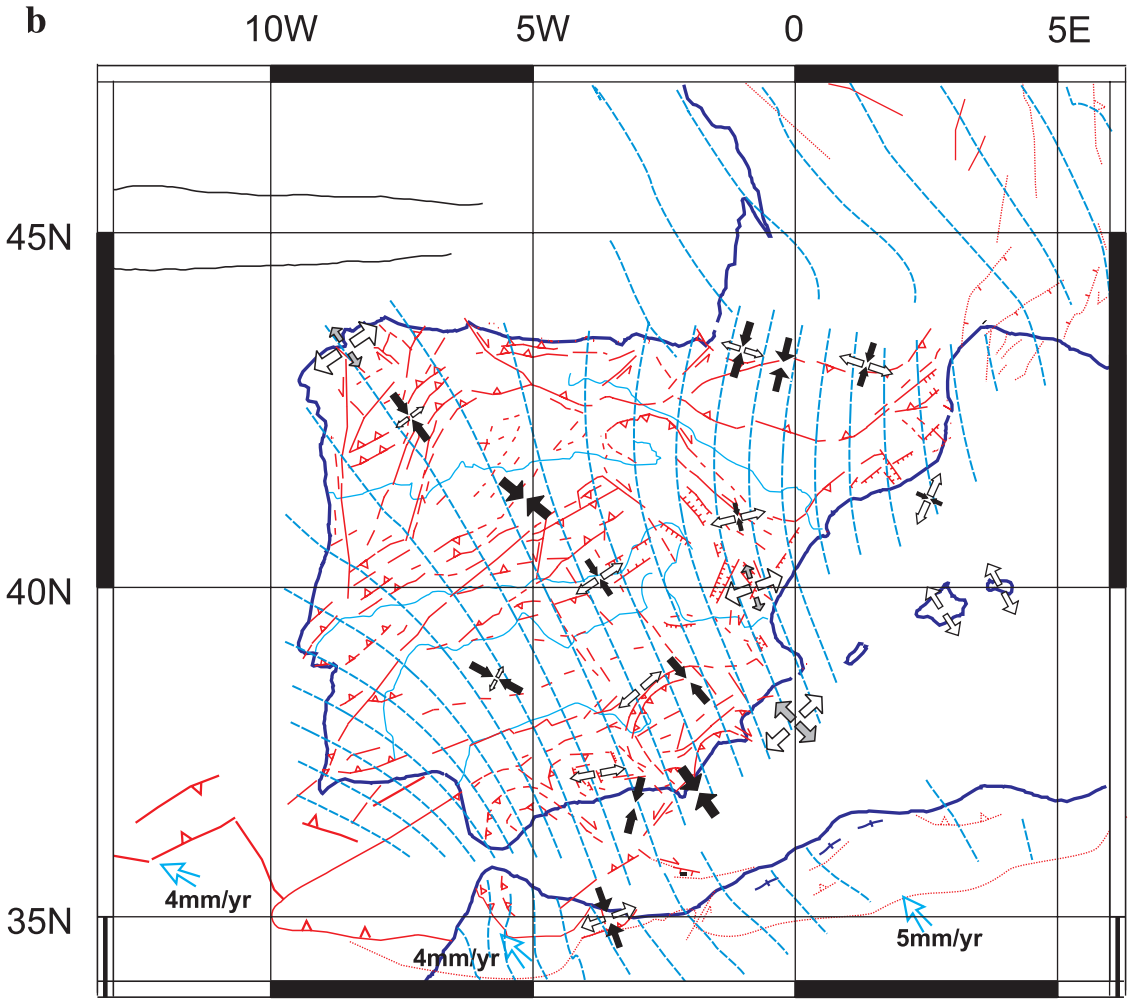

Figure 4. (continued)

have been carried out in the last few years as well as a considerable number of breakout studies in basins in the peninsula explored for hydrocarbons. At the same time structural field studies, till recent times primarily focusing on the Variscan structures in the northern and northwestern peninsula, are now increasingly addressing the record of neotectonics in these areas. Recently, newly available stress indicator data for Iberia [*Ribeiro et al.*, 1996; *Jurado and Mueller*, 1997; *de Vicente et al.*, 1996; *Herraiz et al.*, 1996; *SIGMA*, 1998; *Borges et al.*, 2001] have filled the gap in information on the present-day state of stress of data of the Iberian Peninsula, as is apparent from the database for the World Stress Map [*Zoback*, 1992].

[17] Inspection of Figure 4b demonstrates the presence of a consistently oriented intraplate stress field in South and Central Iberia, with variations in orientation toward the west and northeast. The stresses set up by the collision between Africa and Eurasia, as well as the ridge push forces induced by spreading in the Atlantic appear to propagate into the interior of Iberia, producing a fanning pattern of stress in the Iberian Peninsula. Detailed field studies of Middle Miocene to Quaternary tectonics [*de Vicente et al.*, 1996] and seismic activity have demonstrated an active phase of inversion in the Madrid Basin. The stress field in the neotectonic period in this region has been relatively consistent with regard to the N140–160E direction of maximum horizontal compression direction (Figure 4b). As proposed by *Andeweg et al.* [1999], the existence of contemporaneous parallel compression and extension in areas as the Madrid Basin [*de Vicente et al.*, 1996] and the Betic Cordillera [*SIGMA*, 1998] might be the result of folding in the upper crust. More detailed studies are presently carried out to get a better understanding of the relation between focal depth, focal mechanism and location.

5. Present-Day Topography and Gravity

[18] The topography of Iberia displays a high elevation of the peninsula with a succession of highs and lows trending roughly NE-SW in the interior (see Figure 5a). Inspection of the topographic map (Figure 5a) shows that the topography of a large part of Iberia (the area west of 357° and north of 37°) is characterized on a first-order scale by an alternating

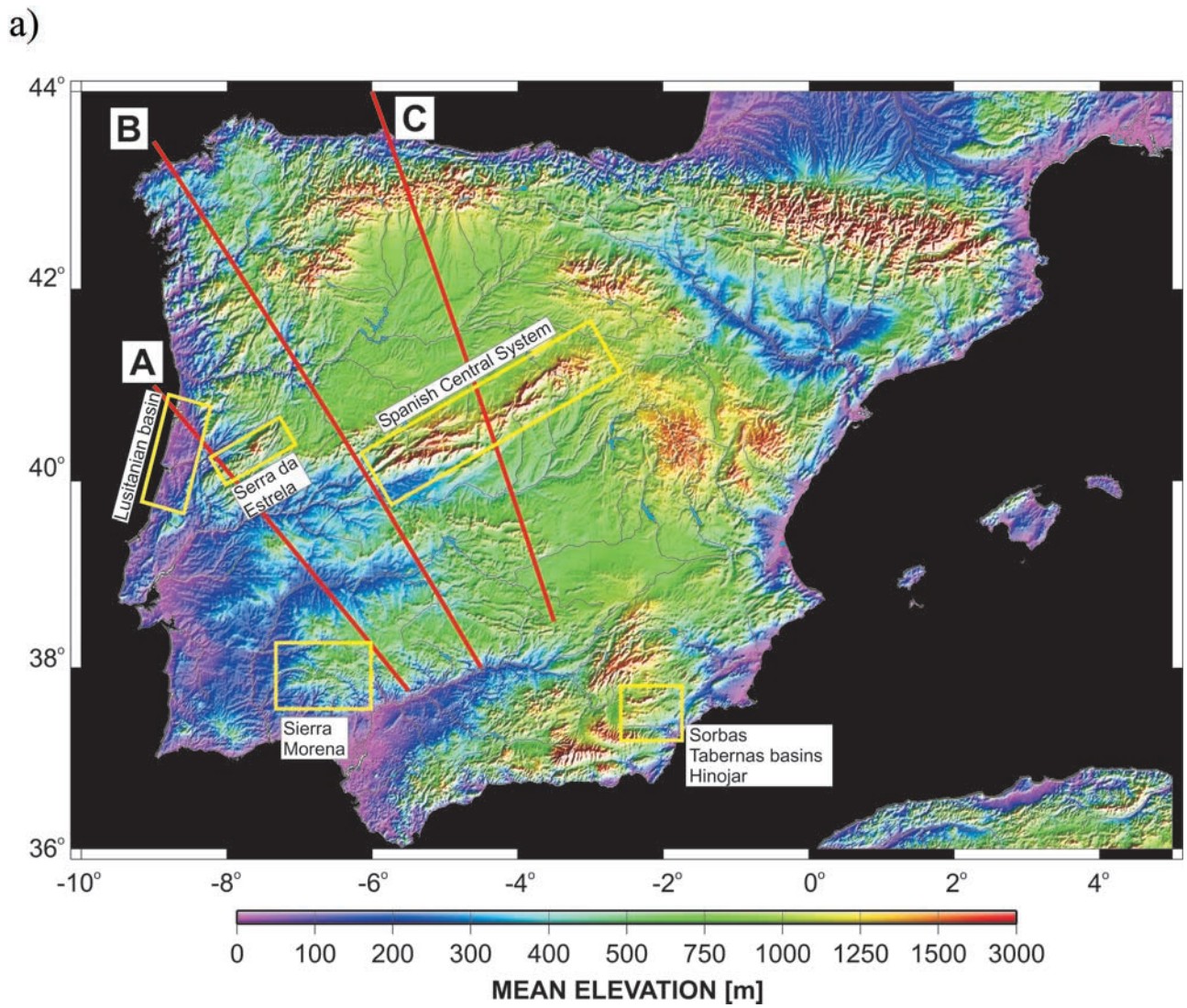

Figure 5. (a) Large-scale topography of Iberia (data from GTOPO30). Boxes refer to location of sites sampled for quantitative subsidence analyses and fission track analysis (see Figure 3). A, B, C mark locations of profiles displayed in Figure 6. (b) Bouguer gravity map of Iberia [*Mezcua et al.*, 1996].

series of E-W to NE-SW trending mountain ranges and river basins. From northwest to southeast this series consists of the Miño river, the Cantabrian/Leon mountains, the Duero-Douro river basin, the Central System, the Tajo river basin, the Toledo mountains, the Guadiana River and the Sierra Morena. The topographic highs and lows are oriented perpendicular to the main axis of present-day intraplate compression in Iberia (Figure 4b).

[19] Similar trends can be observed in the Bouguer gravity map (Figure 5b). As discussed above, the lithosphere of Iberia, although largely of Variscan age, has been subject to subsequent intraplate deformation. The orientation of the anomalously high areas and the magnitude of the post-Miocene vertical motions suggest that the most recent phase of intraplate deformation has exerted a first-order control on the present topographic configuration. The alternating series of topographic highs and lows is more clearly demonstrated in Figure 6a, which shows three topography and Bouguer gravity anomaly profiles transecting Iberia (locations are shown in Figures 5a and 5b). The profiles show a close relationship between magnitude of the gravity anomalies and the makeup of the lithospheric and crustal structure of Iberia.

[20] Variations in Bouguer gravity anomalies reflect the long wavelength variations of the geometry of deep intralithospheric density interfaces, such as the Moho boundary [*Cloetingh and Burov*, 1996]. The wavelength of the Bouguer gravity anomaly thus mirrors the spatial scale of mantle lithosphere deformation. Consequently, the existence of a correlation between periodic long-wavelength Bouguer gravity anomaly and topography indicates the presence of whole-crustal and mantle lithosphere folding, whereas the lack of such correlation is in support of decoupled folding [*Cloetingh et al.*, 1999].

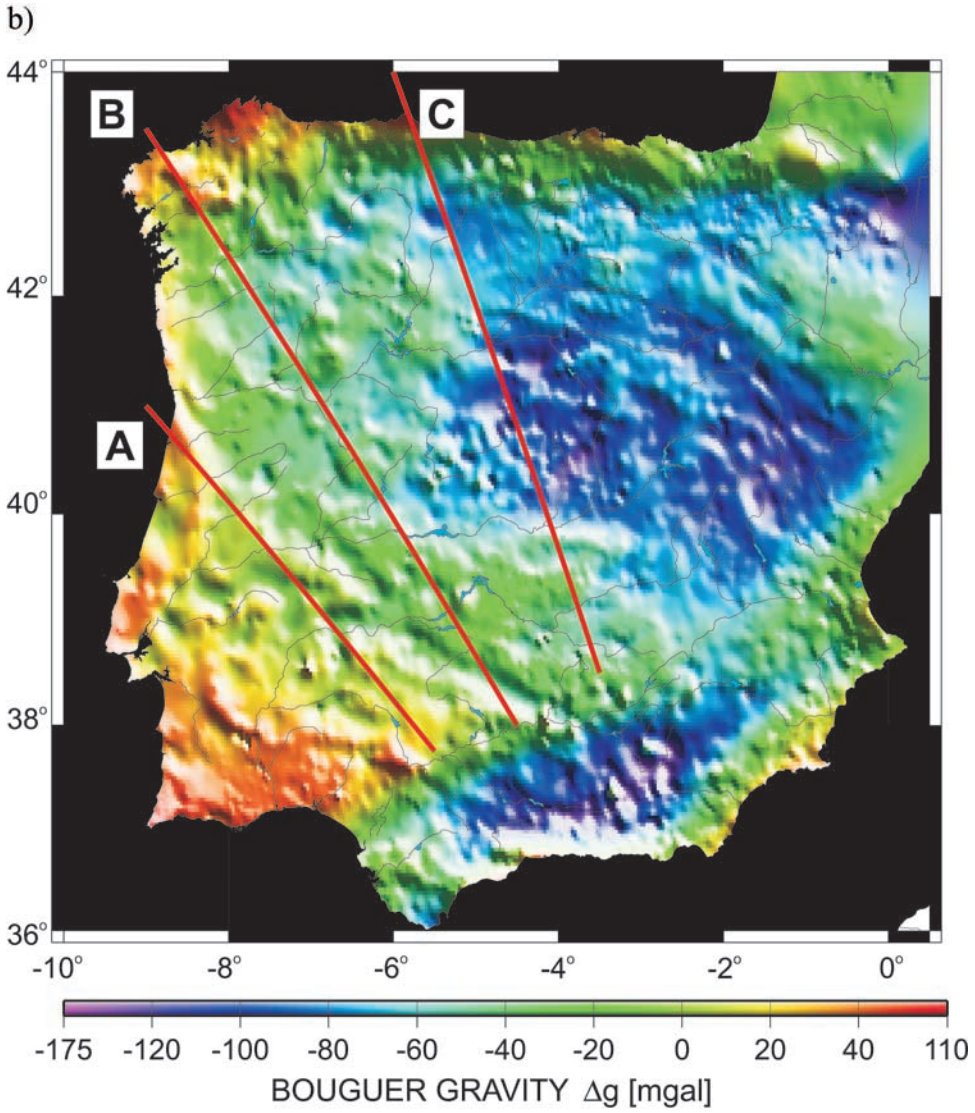

Figure 5. (continued)

[21] Results of a spectral analysis reveal the presence of a dominant wavelength of 200 (±50) km in both the topographic and gravity undulations along profiles A and B (Figure 6b). The power spectra for the gravity also show a large wavelength of at least 500 km, which probably reflects the high average elevated base level of Iberia, with a steep contrast at the borders of Iberia between elevated continental topography and deep oceanic basins. There is no conclusive evidence from seismic tomography for a perturbed upper mantle under Iberia [*Wortel and Spakman*, 2000]. A key question therefore remains whether the high average elevation of Iberia is due to a deep-seated asthenospheric low density source associated with large-scale thermal anomaly reflected in this very long wavelength gravity signal (wavelength longer than 500 km).

[22] The presence of dominant long-wavelength undulations in both topography and gravity has been observed in other intracontinental areas around the world, for instance in central Asia [*Burov and Molnar*, 1998] and in Brittany [*Bonnet et al.*, 2000], and has been explained by these authors as stress induced folding of the continental lithosphere. This folding mode of intracontinental deformation appears to be more important in the large-scale deformation of continental lithosphere than till hitherto thought [*Cloetingh et al.*, 1999].

6. Numerical Models for Lithospheric Folding

[23] The hybrid (finite element/finite differences) explicit code Paravoz [*Poliakov et al.*, 1993] in the version modified by *Burov et al.* [1998] and *Burov and Poliakov* [2001] used in this study allows for direct implementation of various possible geodynamic scenarios. We can, for example, directly introduce lithological and rheological structures derived from seismic and gravity profiles and from thermal and rock mechanics data, using known horizontal convergence rates as the boundary conditions (Figure 7).

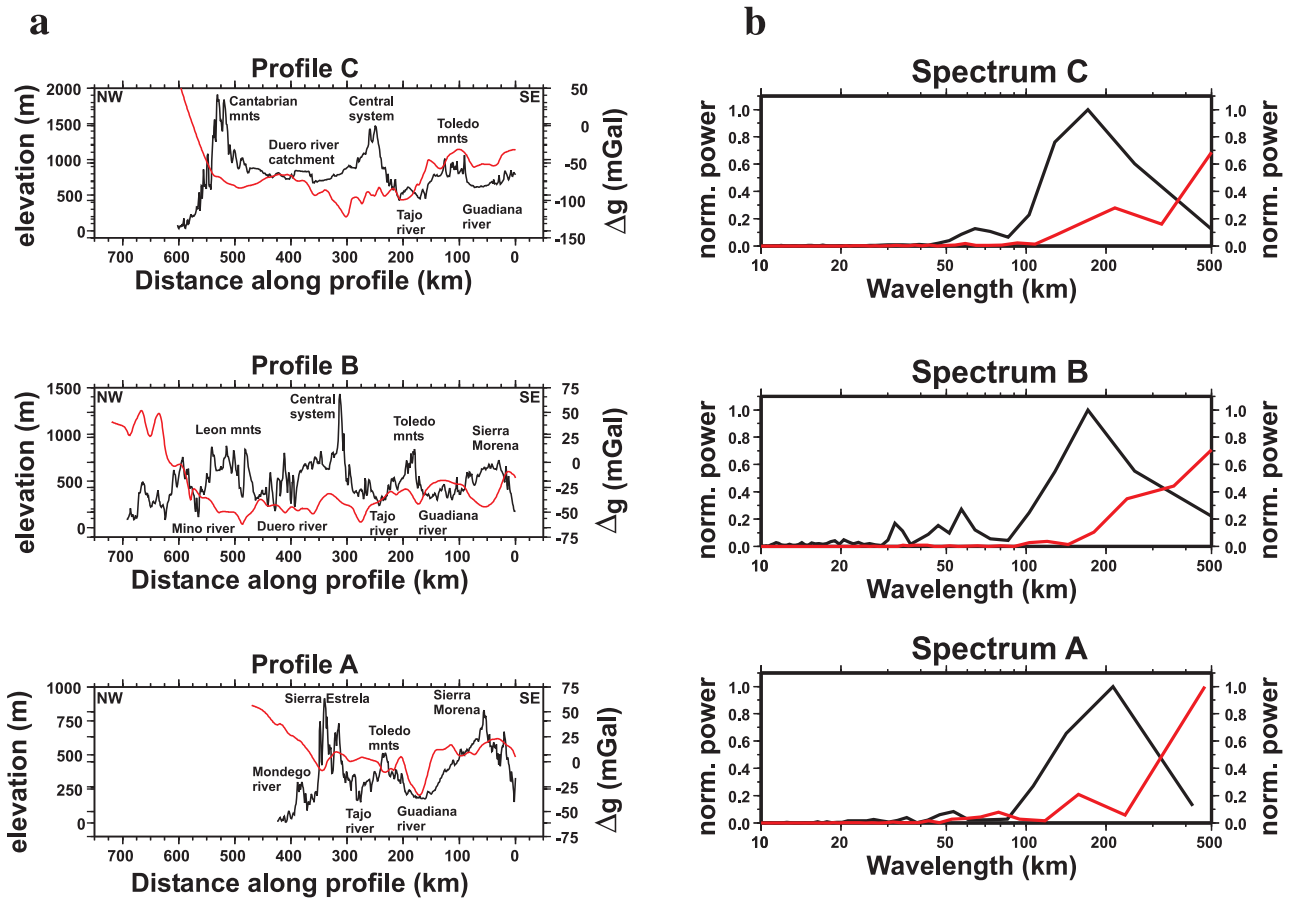

Figure 6. (a) Profiles of topography (black lines) and Bouguer gravity anomalies (red lines). See Figure 5 for profile locations. (b) Normalized power spectra of the topographic profiles (black lines) and the Bouguer gravity anomaly profiles (red lines).

[24] Paravoz is an explicit time-marching Lagrangian code, which is based on the algorithm proposed by *Cundall* [1989] for his FLAC code. This algorithm and its geophysical implementations were described in detail in a number of recent publications [*Poliakov et al.*, 1993; *Burov and Molnar*, 1998; *Burov et al.*, 1998; *Burov and Guillou-Frottier*, 1999; *Cloetingh et al.*, 1999; *Burov and Poliakov*, 2001]. Here we only briefly review some of its most important features.

6.1. The Equations Solved

[25] The code solves the Newtonian equations of motion in a continuum mechanics formulation coupled with heat transport and surface erosion equations:

$$\rho\frac{\partial v_i}{\partial t}-\frac{\partial \sigma_{ij}}{\partial x_j}-\rho g_i=0,$$

$$div(k\nabla T)-\rho C_p\frac{\partial T}{\partial t}+H=\mathrm{v}\nabla T,$$

$$div(k_e\nabla h)-\frac{\partial h}{\partial t}=0,$$

where v_i are respectively components of the velocity vector and **v** is the velocity tensor, σ_{ij} is stress tensor components, x_j are coordinate vector components, g_j are the components of the gravity vector, and ρ is the density. T is temperature, the parameter C_p is the specific heat, **k** is the thermal conductivity tensor, H is the radiogenic heat production per unit volume (here we use the commonly inferred values adopted, for example, as given by *Burov et al.* [1998]), k_e is the coefficient of erosion, and h is the surface topography. The Lagrangian mesh moves with the material, and at each time step the new positions of the mesh grid nodes are calculated from the current velocity field and updated in large strain mode accounting for stress axis rotation. Paravoz can handle rheologically complex behaviors, including localization and propagation of non-predefined faults (shear bands), power law creep and various kinds of strain softening and work hardening behaviors. The modified version of Paravoz allows the incorporation of the erosion/sedimentation models employed by *Burov and Cloetingh* [1997], rheological and lithological models similar to that of *Burov and Cloetingh* [1997], and an initial temperature field for continental lithosphere [*Burov and Diament*, 1995].

6.2. Rheology and Physical Properties

[26] Brittle-elasto-ductile nonlinear rheology is assumed for all materials (Table 1). The crustal and sedimentary

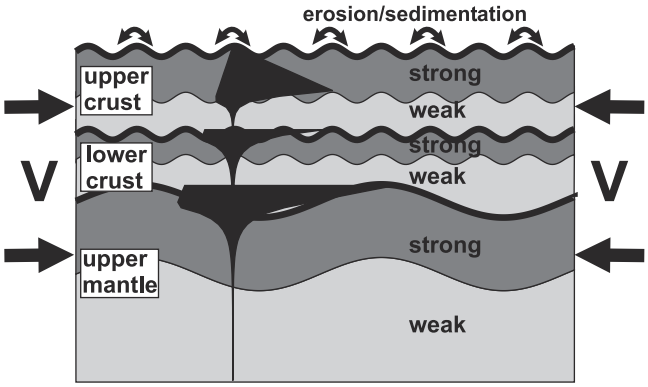

Figure 7. Model setup: v is horizontal shortening velocity; upper crust, lower crust and mantle layers are defined via corresponding rheologies and physical properties (see text). A typical strength profile (in black) for decoupled crust and upper mantle lithosphere adopting a quartz-diorite-olivine rheology is shown for reference.

segment of the lithosphere is represented by a quartz-dominated lithology; the mantle lithosphere is represented by an olivine-dominated lithology. The rheological parameters (elastic moduli, ductile creep material constants, activation energies and power exponents) used here are the same as given by *Burov et al.* [1998]. The brittle part is approximated by Mohr-Coulomb plasticity with friction angle 30° and cohesion of 20 MPa for all materials except sediments, which have smaller cohesion of 5 MPa. The densities are 2300, 2700, 2800, 3330, and 3250 kg/m^3 for the sediment, upper crust, lower crust, mantle and asthenosphere, respectively. The thermal conductivities are 1.6 W m^{-1} K^{-1}, 2.5 W m^{-1} K^{-1}, 2 W m^{-1} K^{-1}, 3.5 W m^{-1} K^{-1}, 3.5 W m^{-1} K^{-1} for the sediment, upper crust, lower crust, mantle, and asthenosphere, respectively. The thermal expansion coefficient used is 3.1×10^{-5} K^{-1}. These values are averages of the range of values presented in a compilation by *Turcotte and Schubert* [1982].

6.3. Surface Processes

[27] We used linear diffusion erosion for the short-range surface processes and flat deposition outside the elevated topography range [*Avouac and Burov*, 1996]. The adopted coefficient of erosion, k_e, is scale-dependent and varies from 0 to 8000 m^2/yr to keep the basins filled with sediments.

6.4. Boundary Conditions

[28] The lateral boundary conditions are prescribed in velocities. We assume free surface on the top and Winkler restoring forces on the bottom of the model. The Winkler restoring force is equivalent to isostatic buoyancy forces used for lithospheric scale models to simulate lithosphere-asthenosphere interactions. It implies a vertical restoring force proportional to vertical displacement of the lower boundary of the model. The coefficient of the proportionality is given by the isostatic condition for the density contrast at the bottom interface of the model. In numerical models the Winkler forces are implemented by a series of ideal elastic springs attached to the bottom of the model. At the upper surface of the model a free surface boundary condition is implemented.

6.5. Setup of Numerical Experiments

[29] The initial thermal structure was imposed using a conventional thermal distribution for a specified thermotectonic age [*Burov et al.*, 1998]. We have carried out a set of numerical experiments employing representative scenarios corresponding to two end member thermal structures of the Iberian lithosphere. The "hot" end-member case has a thermal age of 120 Ma, corresponding to Mesozoic rifting of Iberia [*Van Wees et al.*, 1998], and has a thermal thickness of 250 km. The "cold" end-member case has a thermal age of 350 Ma, corresponding to Variscan deformation of Iberia [*Banda*, 1988; *Vegas and Banda*, 1982; *Ordonez Casado et al.*, 2001; *Simancas et al.*, 2001], and has a thermal thickness of 250 km. The concept of thermal age of continental lithosphere is explained by *Burov and Diament* [1995] and *Cloetingh and Burov* [1996]. In our experiments we used the same set of rheological and thermal parameters as in the studies by *Burov et al.* [1998] and *Cloetingh et al.* [1999]. Parameters adopted for brittle-elasto-ductile rheology including quartz-rich upper and diabase lower crust and olivine-controlled mantle are specified in Table 1. The shortening rates used in the numerical experiments correspond to the values commonly inferred from plate motion and plate reconstruction studies for the area (4 mm/yr) [see, e.g., *Dewey et al.*, 1989; *DeMets et al.*, 1994]. The initial crustal thickness was 32 km with 16 km thick upper crust and 16 km thick lower crust. The length of the numerical box was 1500 × 120 km, or 350 × 30 grid elements (Figure 7).

[30] The goal of the experiments is not to reproduce the fine structure of the present-day topography, but to investigate some of the basic controls on the development of the Neogene to present topography of Iberia. This implies in particular to the interplay of large-scale intraplate compression and surface erosion in Iberia.

Table 1. Creep Parameters for Crustal and Upper Mantle Rocks and Minerals[a]

Mineral/Rock	A, Pa^{-n}s^{-1}	H, kJ mol^{-1}	n
Quartzite (dry)	5×10^{-12}	190	3
Diorite (dry)	5.01×10^{-15}	212	2.4
Diabase (dry)	6.31×10^{-20}	276	3.05
Olivine/dunite (dry)[b]	7×10^{-14}	520	3

[a] Parameters of dislocation climb creep $\dot{\varepsilon} = A\sigma^n.\exp(-H/RT)$ for crustal and upper mantle rocks and minerals. The values correspond to the lower bounds on the rock strength [*Brace and Kohlstedt*, 1980; *Carter and Tsenn*, 1987; *Tsenn and Carter*, 1987; *Kirby and Kronenberg*, 1987]. The elastic moduli used for all materials throughout this paper are a Young's modulus E = 0.8 GPa and a Poisson's ratio ν = 0.25. The brittle properties are represented by Mohr-Coulomb plasticity with friction angle 30° and cohesion 20 MPa [*Gerbault et al.*, 1999].

[b] For olivine at $\sigma_1 - \sigma_3 \geq 200$ MPa the Dorn's dislocation glide creep law is used: $\dot{\varepsilon} = \dot{\varepsilon}_0.\exp\left\{-H * [1 - (\sigma_1 - \sigma_3)/\sigma_0]^2/RT\right\}$ where $\dot{\varepsilon}_0 = 5.7 \times 10^{11}$ s^{-1}, $\sigma_0 = 8.5 \times 10^3$ MPa, and H = 535 kJ mol^{-1}.

7. Far-Field Intraplate Deformation in Iberia: Modeling Results

7.1. The 350 Ma Thermotectonic Age, Symmetric Compression, Erosion

[31] The first set of numerical experiments replicates the geotectonic situation for the westernmost profile experiencing the combined effects from Africa-Europe collision on the south and the Atlantic ridge push in the northwestern segment of the cross section. The models incorporate symmetric shortening, during 20 Myr, of 350 Myr old lithosphere subjected to simultaneous erosion (~3 km of erosion during the model period, which roughly corresponds to the fission track data [*Stapel*, 1999; *De Bruijne and Andriessen*, 2002]. The results (Figure 8a) demonstrate the development of two superimposed large deformational wavelengths, the largest of which is about 350–420 km and the shortest is about 180–200 km. Simultaneously one very short wavelength of 50–60 km develops, apparently resulting from folding and faulting in the uppermost crust, with a fault spacing largely controlled by the thickness of the brittle layer. The very long wavelengths of 350–420 km are not very well expressed in the surface topography as the latter is strongly modified by simultaneous erosion and sedimentation, but are very clearly seen in the displacement velocity patterns and in the geometry of the subsurface layers. The predicted topography patterns with wavelengths of 180–200 km resemble those actually observed (Figures 5 and 6). The presence of two different large wavelengths of deformation indicates partly coupled and partly decoupled folding (described by *Cloetingh et al.* [1999]). In most cases it is difficult to discriminate between folding of the lower crust and upper crust, as their folding wavelengths are quite comparable. Furthermore, the lower crustal folding will not be well expressed in the gravity signal due to insufficient density contrast with the upper crust. We therefore only discriminate between crustal and mantle folding. A partial crustal-mantle coupling can be observed in some plate segments, due to a strong deformation of the upper crust, which is transmitted to the mantle layer. At the same time, the crust-mantle decoupling results in anti-phase folding of the crustal and mantle lithosphere, in which areas of maximum uplift of the crustal basement are laterally shifted with respect to those of maximum mantle depression. Although this geometrically resembles boudinage, it is produced by contra-phase folding of two competent layers. This geometry might lead to incorrect estimates of lithospheric strength. The induced amplitude of the mantle depressions roughly correspond to those expected for local isostatic compensation of the overlying topography, traditionally interpreted in terms of low lithospheric strength. For the short-wavelength upper crustal mode of deformation (wavelength of 50–60 km) the numerical resolution of the problem is just about the limit of resolution for this wavelength (4 elements per crustal layer). To address the resolution problem, we have carried out a number of numerical simulations with double resolution (Figure 8b). These basically reproduce the same wavelength and allow to resolve upper crustal faulting occurring at about 50 and 200 km spacing, consistent with observations (see Figure 6), and high strain rate zones at the crustal/mantle and mantle/asthenosphere boundaries, demonstrating decoupling of the competent lithospheric layers from the weak ductile matrix.

[32] Note that the induced folding patterns display some asymmetry since folding itself is an unstable process. Folding of nonlinear layers is even more unstable, especially at large strains. Such lateral variations of both folding amplitude and wavelength were previously demonstrated in a number of analytical and numerical studies [e.g., *Hunt et al.*, 1996; *Cloetingh et al.*, 1999].

7.2. The 350 Ma Thermotectonic Age, Symmetric Compression, No Erosion

[33] As was pointed out by *Avouac and Burov* [1996], syndeformational erosion coupled with tectonic processes may accelerate localization and then stabilize the evolution of the tectonic deformation. However, if the erosion is too rapid, it may just wipe out all newly created topography and influence the wavelength of folding. For this reason, a series of experiments without erosion were implemented to test the relative importance of simultaneously operating surface processes during intraplate deformation in the Iberian lithosphere. In particular, to assess the importance of the interplay of folding and surface processes, we have repeated the previous experiments without erosion (Figure 8c). A comparison of the results demonstrates that erosion tends to suppress shorter (50–60 km) wavelengths of deformation, but leaves intact the longer wavelengths. It can also be observed that the erosion accelerates vertical uplift rates. Both numerical experiments produce compatible vertical topography amplitudes on the same time scale. However, they differ in the sense that in the erosional case the erosion rate should be added to the surface uplift rate, thus yielding rock uplift rates several times higher than predicted in the absence of erosion.

7.3. The 350 Ma Thermotectonic Age, Asymmetric Compression, Erosion

[34] The second set of experiments with a compressional stress regime initiated at 50 Ma corresponds to the central and the eastern profiles, experiencing the influence from the push exerted by ridge-push and the closure of the Bay of Biscay (starting at 50 Ma) at the northern border of Iberia (Figure 8d). It is analogous to the previous experiments with the difference that the shortening is applied only on the northern side of the plate whereas the southern margin was kept fixed. The folding patterns demonstrate a modest lateral variation of the deformation wavelengths, which are slightly shorter in the south and longer in the north of Iberia.

7.4. The 350 Ma Thermotectonic Age, Asymmetric Compression, No Erosion

[35] This set of experiments repeats the previous one but with no erosion included (Figure 8e). Note that the short wavelength of deformation is well present in this case and that the surface geometry basically resembles some typical

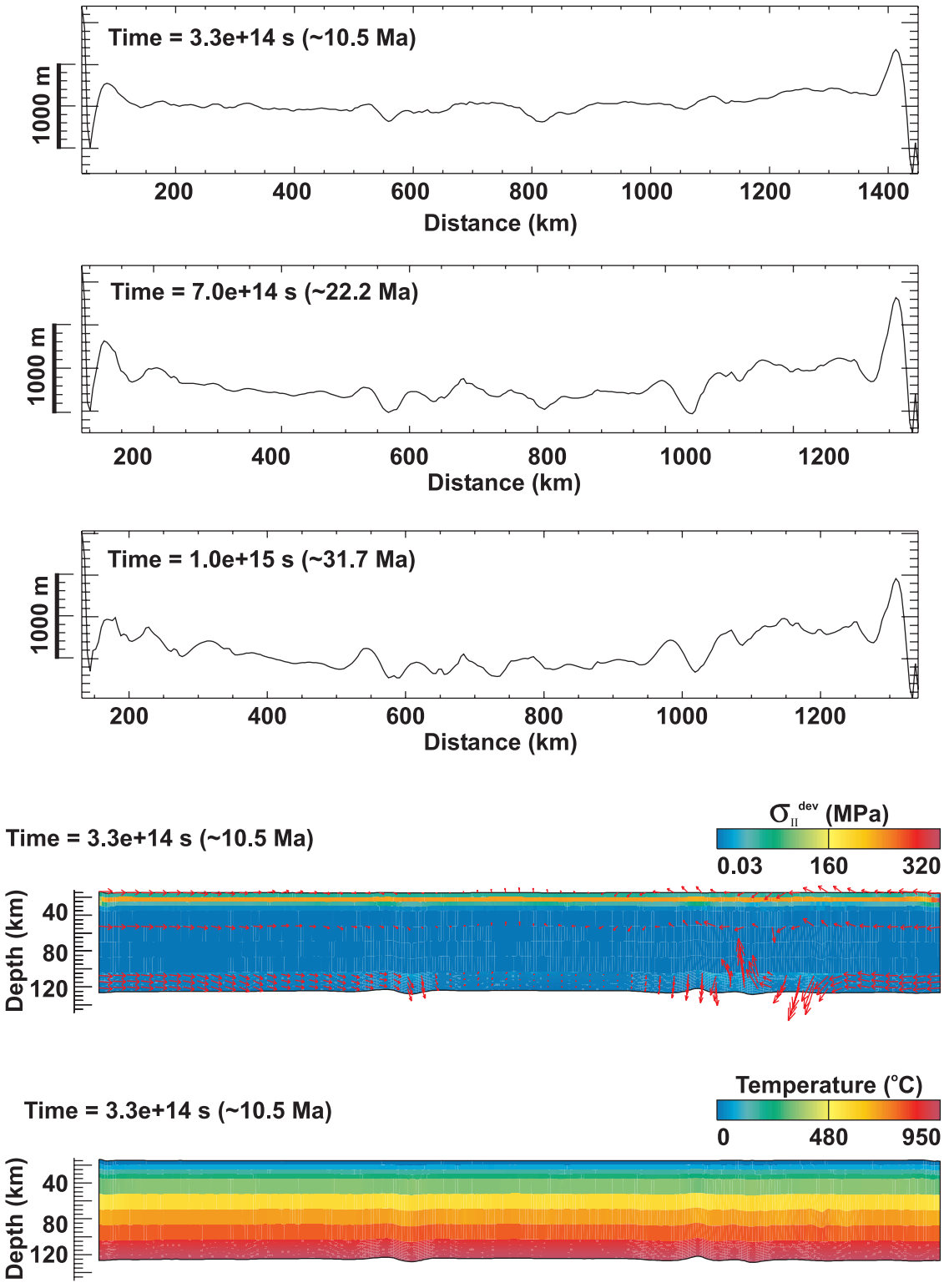

Figure 8a. Results of numerical experiments for symmetrical shortening of continental lithosphere with a thermotectonic age of 350 Ma and a shortening rate of 4 mm/yr (equivalent to 2 mm/yr on each side of the box). High erosion rate (scale-dependent coefficient of erosion k_e = 5000 m^2/yr). Topography at three time steps (upper three panels), shear stress and velocity field (indicated by red arrows) (middle panel) and temperature field (bottom panel). Note different characteristic wavelengths of crustal and mantle folding (see text). Printed times designate time from start of onset of deformation in the model runs. Left- and right-hand side panels in Figures 8 to 10 correspond to north and south ends of investigated profile lines through Iberia (Figure 5).

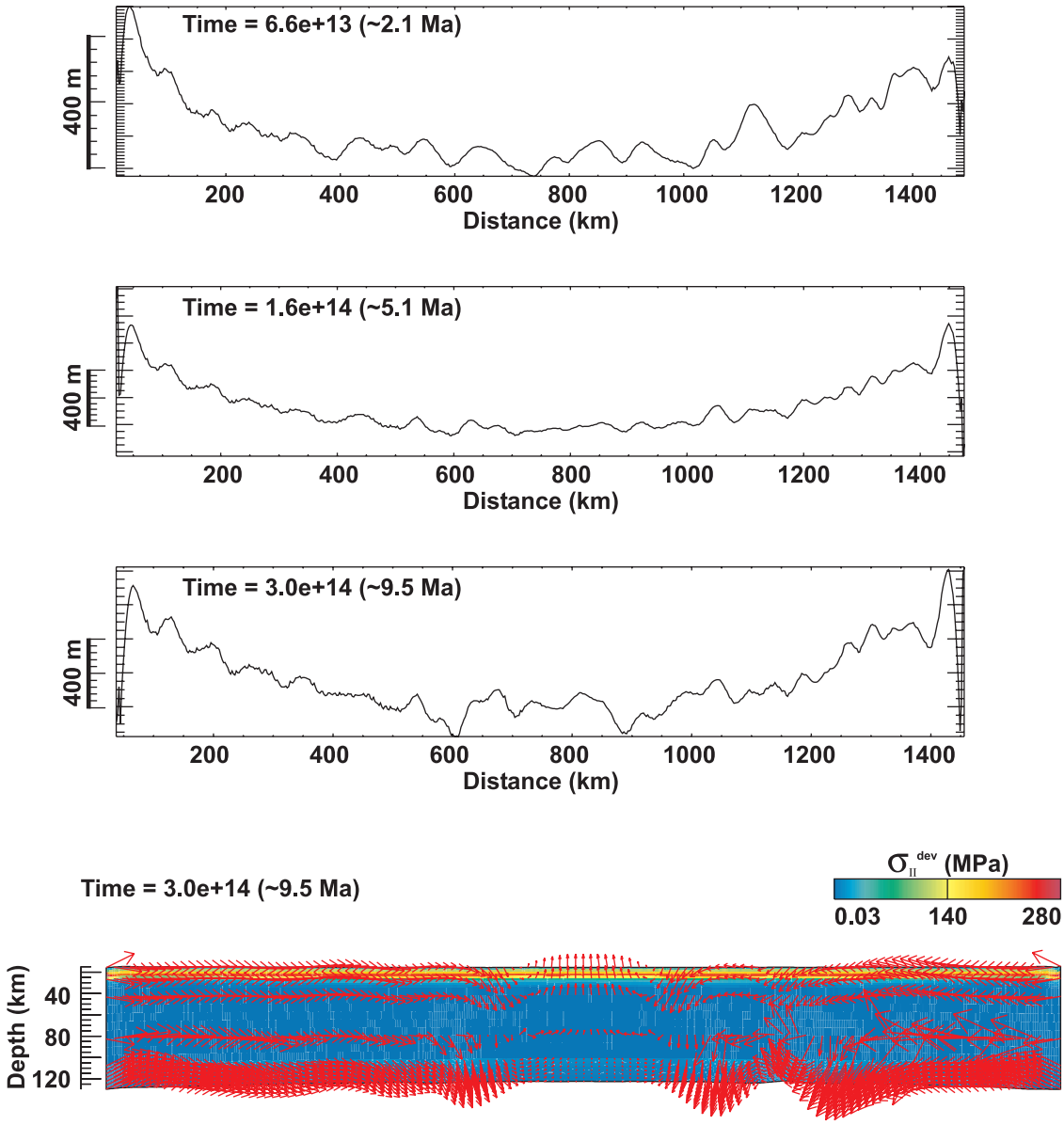

Figure 8b. Results of a numerical high-resolution experiment corresponding to the same scenario as displayed in Figure 8a. This double resolution model allows a better handling of crustal-mantle decoupling and faulting. Topography at three time steps (upper three panels), and shear stress and velocity field (indicated by red arrows) (bottom panel). Note "boudinage" like geometry of folding of the competent layers. Also note the lateral localized shear zones of high strain rate at the crustal-mantle and mantle-asthenosphere boundaries indicating decoupling at northern and southern borders of Iberia. The difference in the predicted topography displayed in Figures 8a and 8b relates to impossibility to obtain exactly simultaneous snapshots as result of different time steps used by the numerical code. This is inherent to the dynamic time step adjustment capability of the code, which allows for reduction of the (substantial) calculation time involved.

features of the Iberian topography. The longest folding wavelength appears to be the same as in the previous case.

7.5. The 120 Ma Thermotectonic Age, Symmetric Compression, Erosion

[36] The third set of experiments (Figure 9) considers a thermally younger lithosphere with a thermotectonic age (that is the time elapsed since the last major thermal event) of 120 Ma. At this time the eastern margin of Iberia underwent major extension and reheating [*Van Wees et al.*, 1998]. At the same time stratigraphic studies of the Duero basin indicate that it was only mildly affected by this phase of reheating suggesting that the western part of Iberia did not underwent any major reheating at that time. Figure 9 shows that in this

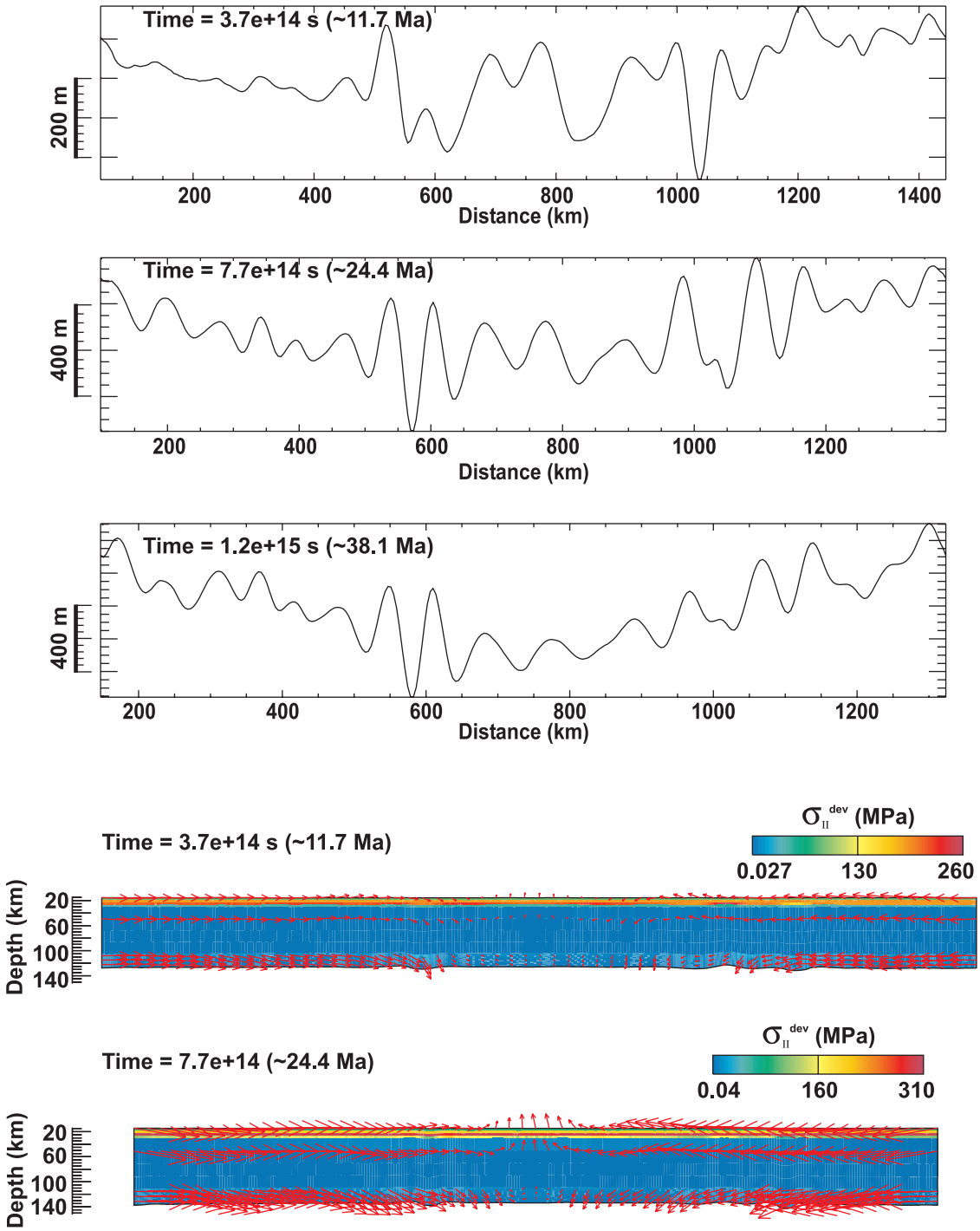

Figure 8c. Results of the same numerical experiment as presented in Figure 8a, but with a zero erosion rate. Topography at three time steps (upper three panels), and the shear stress and velocity field (indicated by red arrows) for two successive time steps (bottom two panels). Note the enhanced development of the shorter wavelengths, resulting in higher amplitude of short wavelength topography and basins.

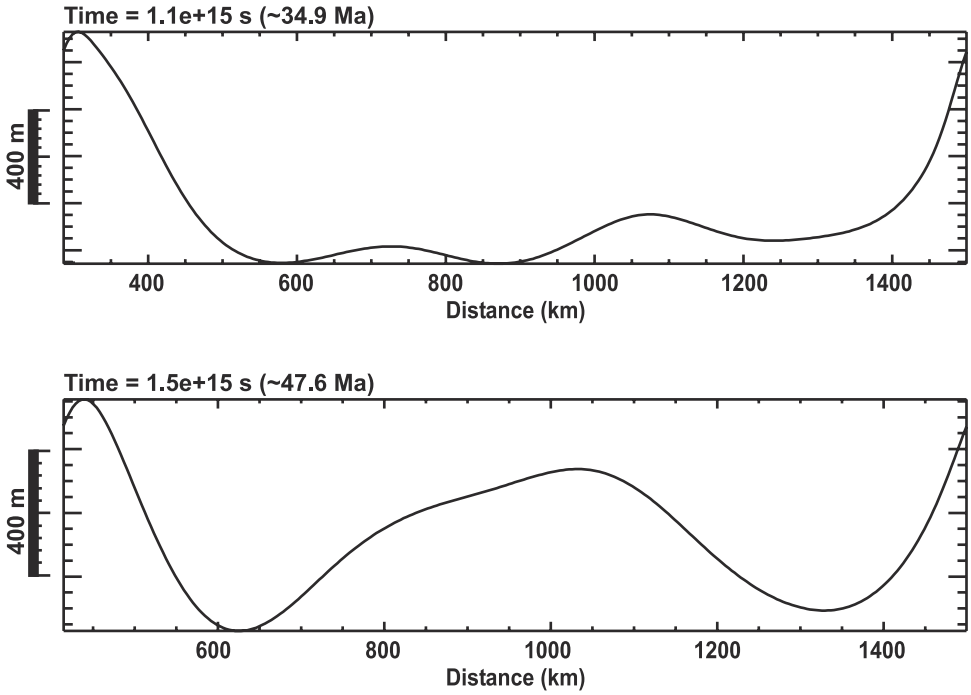

Figure 8d. Results of a numerical experiment on asymmetric shortening of a 350 Ma lithosphere (v = 4 mm/yr) on the northern side. High erosion rate (scale-dependent coefficient of erosion k_e = 5000 m^2/yr). Note that for a higher shortening rate at one side of the model and a similar erosion coefficient, the erosion rates tend to be higher, leading to suppression of the short wavelengths in topography. This is displayed for two successive time steps.

case the folding instability develops only in the cold upper crustal domain and that the deformation is concentrated at the boundaries of the plate. It is thus likely that such a weak rheological structure is not plausible in the particular tectonic configuration of Iberia [*Faccenna et al.*, 2001].

7.6. Northward Increasing Lithospheric Strength (Thermotectonic Age Increases From 120 Ma to 350 Ma), Symmetric, Erosion

[37] A major question is whether the amount of shortening induced by the Africa-Europe collision has been primarily accommodated in the Alboran block characterized by relatively high heat flow [*Fernandez et al.*, 1998] and major thermal rejuvenation associated with Upper Jurassic to Early Cretaceous rifting. Such an inferred weak zone could have a strong effect on stress propagation due to forces exerted at the southern boundary of this Alboran block on the adjacent stronger Iberian lithosphere. To investigate this scenario, we have constructed a model involving an important lateral variation in strength. These models (Figure 10) aim at testing the hypothesis of lateral variations in the thermal state of the lithosphere, as suggested by surface heat flux data indicating an increase of the heat flow to the south [*Fernandez et al.*, 1998]. To account for this scenario, we introduced a lateral variation in the thermal field, which corresponds to a 120 Ma thermotectonic age in the 500 km long southern segment of the lithosphere and a 350 Ma thermotectonic age in the 1000 km long northern segment. The general basement deformation patterns are similar to those produced in the experiments with laterally homogeneous lithosphere, but at depth the model demonstrates more intensive mantle and crustal folding in the southern part (with wavelengths of about 320–350 km on the south and 420 km to the north). Mantle folding in the southern part of the Iberian plate results in localization of the deformation in a single down warped mega fold resembling subduction patterns inferred from analogue modeling [*Faccenna et al.*, 2001].

8. Discussion

8.1. Spatial Variations in Rheology

[38] The topographic and lithospheric structures predicted by the modeling in the case of Variscan-type lithosphere, are strongly similar to those actually observed. It should be realized that the data available (rheology data, heat flow) only allow for a first-order evaluation of the input rheological profiles and the thermal field. For this reason we have implemented a number of experiments in which we have varied the internal mechanical structure of the lithosphere from those corresponding to thermotectonic ages of 120 Ma to 350 Ma. Irrespective of the actual thermotectonic age of the lithosphere, it appears that the models for continental lithosphere of 350 Ma reproduce very well the overall behavior of the Iberian lithosphere. This result is additionally supported by previous estimates

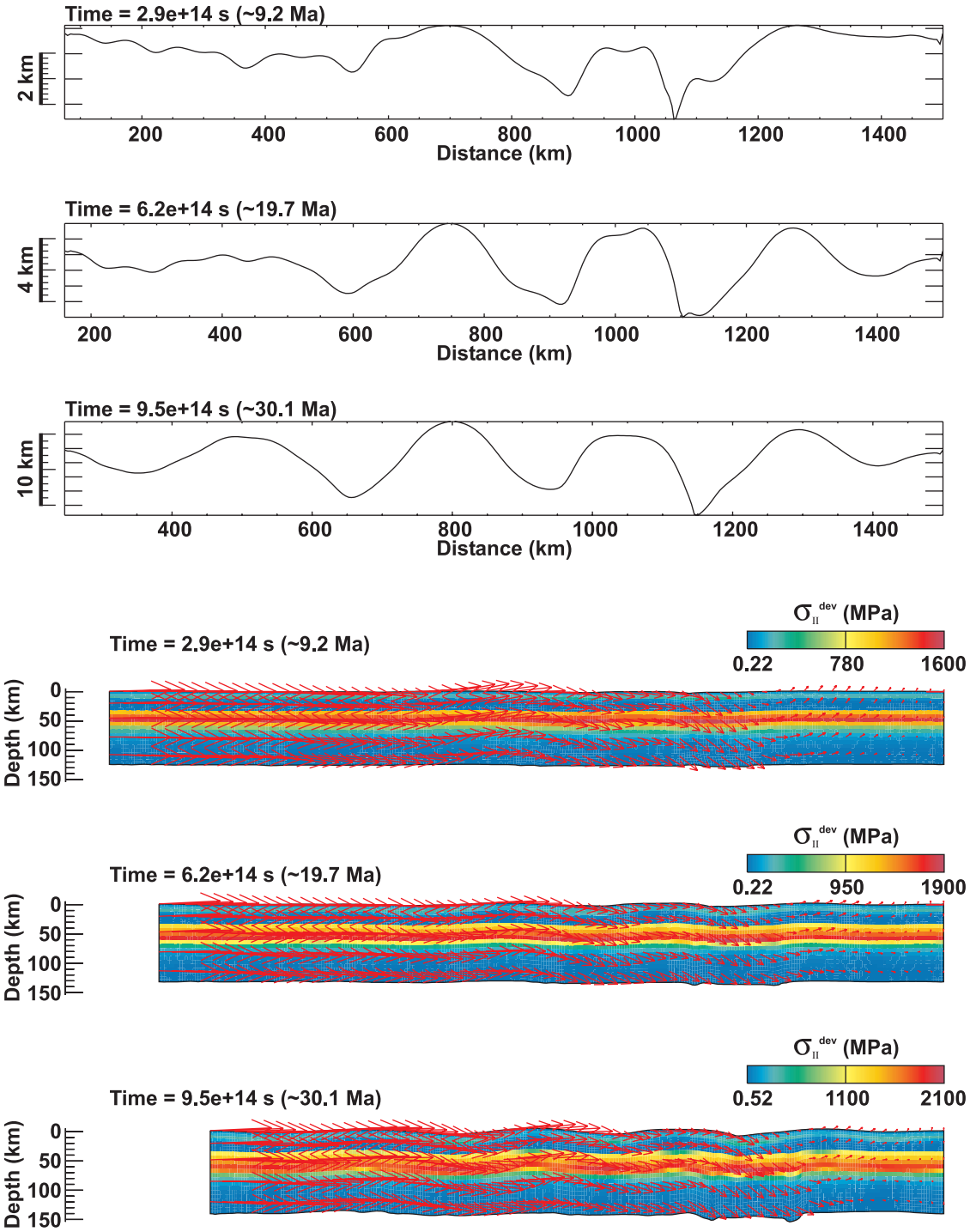

Figure 8e. Results of a numerical experiment on asymmetric shortening of a 350 Ma lithosphere (v = 4 mm/yr) on the northern side. No erosion. Topography at three time steps (upper three panels), and the shear stress and velocity field (indicated by red arrows) for three successive time steps (bottom three panels).

of 30 km for the effective elastic thickness (EET) obtained for the Ebro basin in northeastern Spain [*Gaspar-Escribano et al.*, 2001], which also well corresponds to the theoretical prediction given by *Burov and Diament* [1995] for 350 Ma lithosphere. For central Spain, *Van Wees et al.* [1996] provide a lower bound estimate for the upper crustal EET of only 7 km. This value is somewhat less than the 12–15 km estimate for upper crustal EET, predicted from

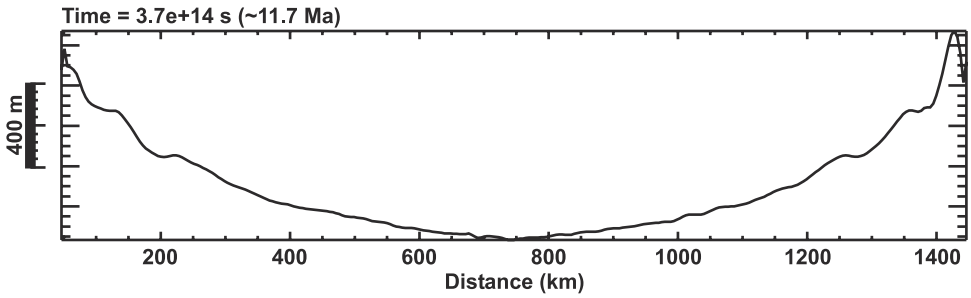

Figure 9. Results of numerical experiments on symmetric shortening of a 120 Ma lithosphere (v = 4 mm/yr), and with an erosion coefficient k_e = 5000 m^2/yr. Striking in the topography is the apparent lack of folding, probably due to a low competence contrast within the lithosphere, also leading to partial localization at the borders of the model.

rheological profiles of the thermal and lithological structure adopted in this paper. Locally, crustal detachment accompanied by brittle deformation in the upper crust and ductile thickening of the lower crust could have played a role in the localization of uplift in the Spanish Central System [*de Bruijne and Andriessen*, 2002].

[39] As pointed out by *Andeweg et al.* [1999], the spatial distribution of present-day seismicity and Quaternary deformation indicates a present amplification of the initial foreland-bulge of the Madrid basin-Spanish Central System due to intraplate compression. Similar conclusions were reached by *Garcia-Castellanos et al.* [2002] on the basis of an integrated analysis of the Betic foreland basin. These authors pointed out that a major amplification of the flexural foreland loading by intraplate compression was required to yield the observed history of basement stress and basement deflection evolution and the adjacent uplift in the Sierra Morena area. The obtained low values of EET estimates in this area (EET = 18 km) are interpreted in terms of flexural decoupling of crust and mantle and/or stress-induced weakening due to horizontal compression. Flexural decoupling is also inferred from structural restorations in the area [*de Vicente et al.*, 1996].

[40] The above observations suggest that the wavelength of deformation increases to the north, which can be explained either by the proximity to the active plate boundaries (Figure 4), or by the hotter thermal state of the lithosphere in the south (Figure 2).

[41] The models used imply basically laterally homogeneous crustal structure. There is no technical difficulty to introduce various lateral variations and preexisting faults in the model [see also *Beekman et al.*, 1996; *Gerbault et al.*, 1999]. As was shown by *Cloetingh et al.* [1999], preexisting crustal faulting and segmentation in general do not have a significant affect on the developing folding wavelength unless these faults crosscut the entire crust and mantle lithosphere.

8.2. Interplay Between Surface Transport and Vertical Motions

[42] As pointed out above, the thermal modeling of fission track data favors a Pliocene phase of simultaneous uplift and erosion rather than a Miocene uplift phase followed by Pliocene erosion [*de Bruijne and Andriessen*, 2002]. This is important, as the erosion following the creation of lithospheric folds will redistribute mass at the surface into the topographic lows, thus enhancing the flexure of the underlying lithosphere. In this context, it should be noted that our modeling approach is by its nature 2-D, whereas drainage patterns characteristic of some of the major rivers of Iberia, including the Tajo, the Duero and the Guadiana rivers, trending in a NE-SW direction, remove sediments out of the plane of cross section toward the coastal areas. A noteworthy feature (see Figure 5a) is the progressive development of the drainage systems toward the Betics, resulting in a fully developed drainage system in the Guadalquivir River, whereas the Duero River only very recently crosscut the coastal topography, establishing an opening of the Duero Basin toward the Atlantic. Numerical experiments of drainage network evolution [*Garcia-Castellanos*, 2002] demonstrate that surface transport processes effectively enhance the tectonically induced large-scale continental topography.

[43] In 2-D (cross section) modeling studies including the one presented above, erosion is often approached as a diffusive process. This technique permits to reproduce the basic effects of surface transport, such as transport from elevated areas to relief depressions and the eventual peniplanation of an initially rough topography. However, diffusivity is not a process-based approach for large-scale transport. In the temperate climatic conditions of Iberia during most of the Tertiary, most of this surface mass transport is undertaken by rivers. River catchments have typically strong 3D asymmetry since their drainage is hierarchically organized to collect the waters and sediment from a widespread area into a single outlet. This property implies that whereas erosion is distributed along a large area of the catchment's headwaters, deposition takes place relatively localized along the lower riverbed and around the river mouth in the Atlantic Ocean and possible intermediate lakes.

[44] The pre-Alpine paleogeography of the Iberian Massif corresponds to a relatively flat topography resulting from the erosional planation during the long period elapsing between the Hercynian and the Alpine orogenies. Vertical

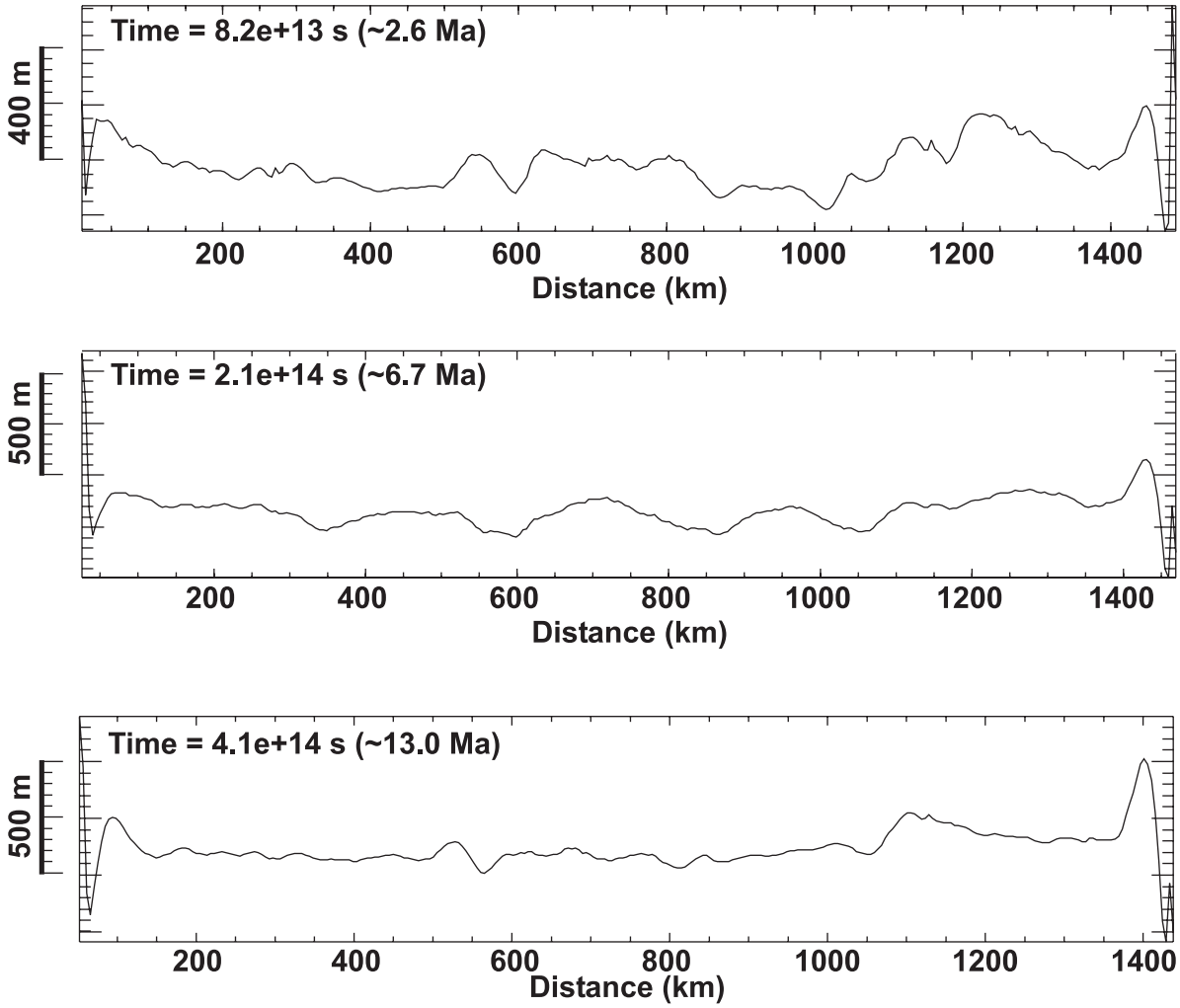
Time = 8.2e+13 s (~2.6 Ma)
400 m
200
400
600
800
1000
1200
1400
Distance (km)
Time = 2.1e+14 s (~6.7 Ma)
500 m
200
400
600
800
1000
1200
1400
Distance (km)
Time = 4.1e+14 s (~13.0 Ma)
500 m
200
400
600
800
1000
1200
1400
Distance (km)

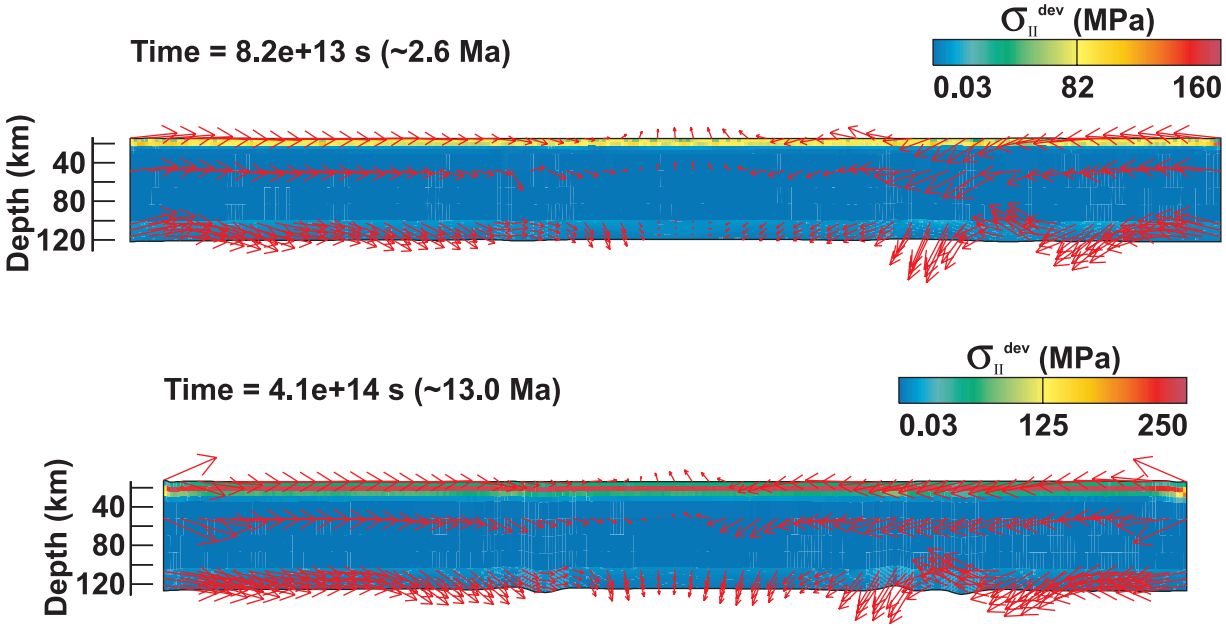
Time = 8.2e+13 s (~2.6 Ma)
σII dev (MPa)
0.03
82
160
Depth (km)
40
80
120
Time = 4.1e+14 s (~13.0 Ma)
σII dev (MPa)
0.03
125
250
Depth (km)
40
80
120

movements modify river profiles and the distribution of drainage basins [e.g., *Kooi and Beaumont*, 1996; *Bonnet et al.*, 1998]. Despite the intrinsic nonlinear nature of drainage networks, moderate vertical movements seem also to be capable to organize the drainage patterns in relatively flat areas where drainage is not well-organized or incised [*Garcia-Castellanos*, 2002].

[45] In the studied region of central and western Iberia, drainage is mostly oriented westward, implying that whereas widespread erosion takes place in the whole region, deposition is restricted to the westernmost edge of the Iberian Peninsula: at the lower part of the valleys and offshore in the Atlantic Ocean. However, the diffusive models used above assume erosion at high areas and deposition at topographic minima along the studied cross sections. Therefore models adopting diffusive transport should be considered as a first-order approximation.

8.3. Lithosphere Folding and Drainage Patterns

[46] To further evaluate the interplay between surface transport and lithospheric folding, we simulate fluvial transport via a drainage network in which runoff water flows along the maximum slope with a sediment transport capacity proportional to slope and water discharge. For the implementation of this approach, which intrinsically predicts planform hierarchical organization of drainage networks, we use the relationships by *Beaumont et al.* [1992], subsequently adopted in several studies [e.g., *Kooi and Beaumont*, 1996; *Braun and Sambridge*, 1997; *Van der Beek and Braun*, 1998]. It should be noted that there is an ongoing discussion on the optimal empirical relationships relating the actual amount of erosion/deposition to slope and water discharge [e.g., *Willgose et al.*, 1991; *Howard et al.*, 1994; *Tucker and Slingerland*, 1995; *Whipple and Tucker*, 1999]. This discussion is of secondary importance for this study, as our analysis focuses on the first-order features of the interplay between fluvial transport and folding, rather than on the properties of fluvial transport themselves. The model applied here incorporates additionally the deposition in topographic minima (lakes) and in the Atlantic Ocean, which allows for modeling closed transport systems where virtually all eroded material is deposited within the model (further details are given by *Garcia-Castellanos* [2002]).

[47] Folding is calculated as the response of a thin homogeneous visco-elastic 2-D (plan form) thin-plate to tectonic loading (horizontal) and surface mass redistribution (vertical load). The equation governing this plate is derived by applying the principle of correspondence between elasticity and visco-elasticity [*Lambeck*, 1983] to the equivalent elastic equation [e.g., *Van Wees and Cloetingh*, 1994]. It should be noted that this approach of the lithospheric rheological behavior is less sophisticated than the ones governing the 2-D (cross sectional) models presented above. Whereas the 2-D models have the full capacity to incorporate a true depth-varying elasto-ductile-viscous rheology, the planform models are restricted to an approximate depth-independent visco-elastic rheology. The planform models, however, are superior to the 2-D models in terms of the treatment of surface transport as well as their capability to address the 3D nature of the lithospheric deformation of Iberia. The cross section and the planform models therefore should be considered as complementary, thus allowing to investigate both the main characteristics of the depth-dependent response of the lithosphere as well as the plan view of the first-order pattern of intraplate deformation and topography evolution.

[48] We have calculated the 3-D response to lithosphere shortening adopting an effective elastic thickness (EET) of 30 km. This value corresponds to a mechanically coupled crust and mantle lithosphere with a thermotectonic age of 350 Ma, and is consistent with results from a flexural analysis of the Ebro Basin in northeastern Spain [*Gaspar-Escribano et al.*, 2001]. A viscous relaxation time of 1.2 Myr is adopted from a recent flexural analysis of the Guadalquivir Basin (southern edge of the Iberian Massif) [*Garcia-Castellanos et al.*, 2002]. The initial configuration of the synthetic models is a flat square continent elevated at 400 m above sea level with a random perturbation between −10 and +10 m. The ocean surrounding this square region is 2000 m deep. The deflection in the boundaries of the model is set to zero. We assume a runoff (water going to the drainage system) distribution of 200 + 300*altitude (m) mm yr^{-1} and adopt standard values for the transport parameters [*Kooi and Beaumont*, 1994, 1996]: constant of river transport capacity $K_f = 0.01$; length scale of fluvial erosion L_{fe} = 120 km (60 km for sediment erosion); length scale of fluvial sedimentation L_{fs} = 25 km.

[49] Figure 11a shows the drainage networks resulting after a period of 12 Ma of N-S directed horizontal compression. For initial random perturbations of the topography lower than ∼20 m, the resultant drainage pattern is clearly controlled by a ∼350 km wavelength of lithospheric folding. A reduction to an EET of 18 km, closer to the values found in the Guadalquivir Basin [*Garcia-Castellanos et al.*, 2002] reduces this characteristic wavelength to 220 km. During the initial stages of compression, the peniplane geometry limits erosion and deposition only to the vicinity of the shoreline, whereas the interior of the continent remains almost unperturbed. The vertical movements associated with this initial mass transport near the shoreline play a role as the necessary perturbations that trigger folding. As a consequence, maximum uplift occurs along the north and south shores, as they are perpendicular to the compression axis.

Figure 10. (opposite) Results of numerical experiments with a laterally varying thermotectonic age, incorporating a 1000 km long segment in the north of Iberia with a thermotectonic age of 350 Ma and a 500 km long segment in the south with a thermotectonic age of 120 Ma. High erosion rate (scale-dependent coefficient of erosion k_e = 5000 m^2/yr). Topography at three time steps (upper three panels), and the shear stress and velocity field (indicated by red arrows) for two successive time steps (bottom two panels). The predicted wavelength is increasing in northward direction away with distance from the African-Europe plate boundary (see Figures 5a and 6a for comparison).

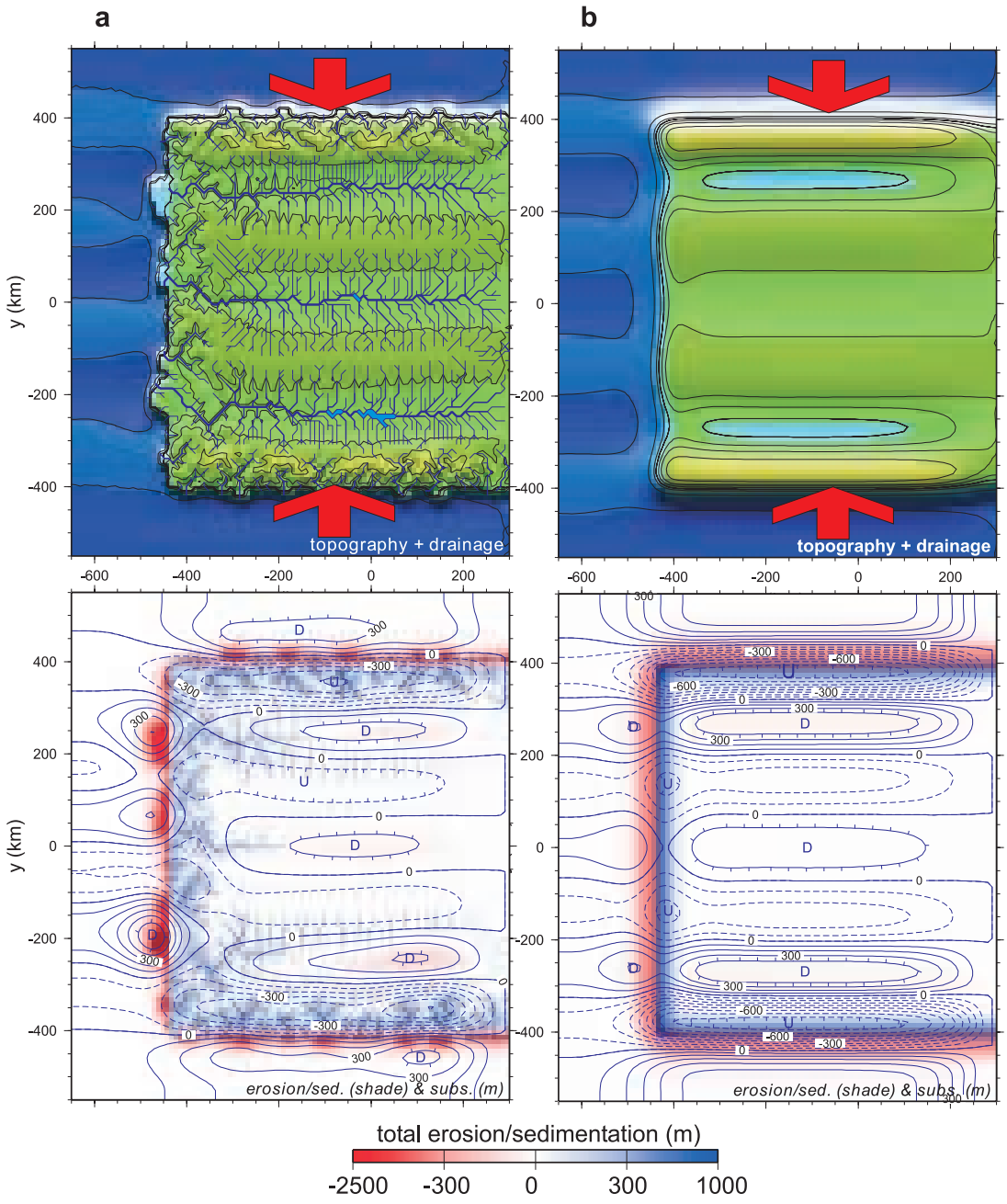

Figure 11. Results of synthetic models, shown in plan view, of the interplay of lithospheric folding and surface erosion and sedimentation processes. The models adopt an initially flat, square-shaped continental geometry with dimensions representative for Iberia. River thickness is proportional to water discharge. Contours indicate vertical motions (m) induced by a 12 Myr duration of N-S oriented compression. Upper panels show topography and drainage networks. Lower panels show accumulated erosion/deposition (shading) and vertical motions (contours labeled in meters). (a) Synthetic model incorporating a superposition of lithospheric folding and fluvial transport through a drainage network. See text for details and specification of model parameters. (b) Synthetic model incorporating a superposition of lithospheric folding and erosional transport by adopting a diffusive model for mass redistribution. The main axes for topographic linear highs and lows predicted by the plan view synthetic models are perpendicular to the main axes of shortening. This corresponds with the actually observed relationship between topography and stress field, with large-scale topographic linear highs and lows perpendicular to the main axis of present-day intraplate compression in Iberia (Figure 2). Note that a NW-SE oriented main axis of shortening (Figure 2) would rotate the main axis of drainage and erosion and sedimentation into a NE-SW orientation, more closely corresponding to the topography of Iberia (see Figure 5a).

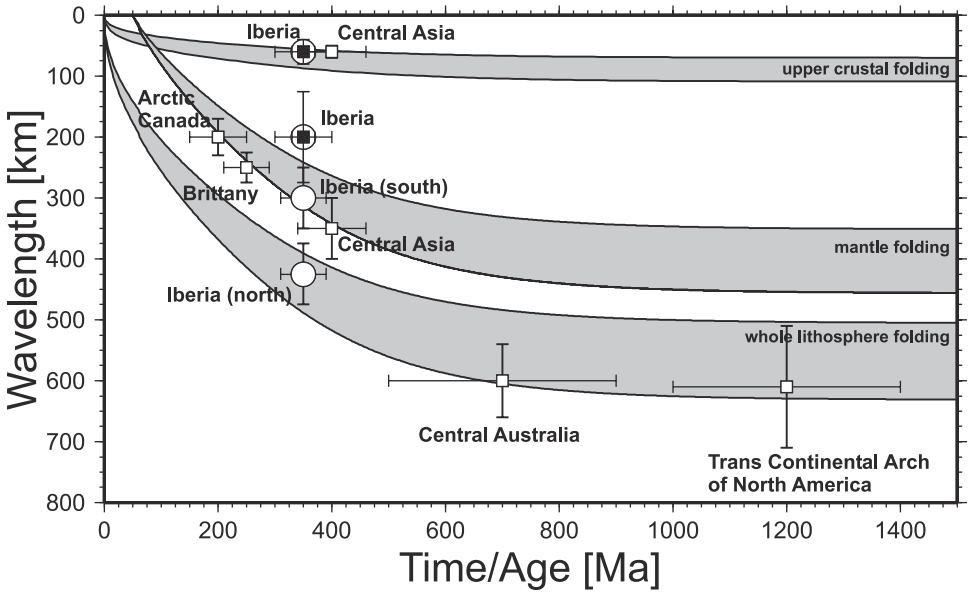

Figure 12. Comparison of observed (solid squares) and modeled (open circles) wavelengths of folding in Iberia with theoretical predictions [*Cloetingh et al.*, 1999] and other estimates (open squares) for wavelengths documented from geological and geophysical studies [*Stephenson and Cloetingh*, 1991; *Lambeck*, 1983; *Ziegler et al.*, 1995; *Nikishin et al.*, 1993; *Bonnet et al.*, 2000]. Note that neotectonic folding of Variscan lithosphere has recently also been documented for Brittany [*Bonnet et al.*, 2000; *Guillocheau*, 2002]. Both Iberia and central Asia are characterized by separate dominant wavelengths for crust and mantle folds, reflecting decoupled modes of lithosphere folding.

[50] Inversely, the organization of drainage has also important effects on the vertical motions. This is illustrated by a comparison of Figure 11a with an identical model where transport is diffusive (Figure 11b), adopting a value of $k_e = 33.0$ m^2/yr. Although we chose the diffusive constant to produce a total transport of sediments similar to the previous model (71.9×10^3 km^3), the hierarchical organization of the drainage pattern has a strong influence on the spatial redistribution of mass. Deposition is localized near the main river mouths and in phase with the vertical motions, since drainage is forced along the E-W trending folding minima (Figure 11a). It therefore accentuates the folding pattern off the west shore, at $x < -420$ km. Instead, a diffusive approach to surface transport does not introduce relevant asymmetries in the x direction (Figure 11b) except for overprinting the folding pattern along the western Atlantic margin of Iberia. Therefore river transport is less efficient in amplifying vertical motions because erosion and sedimentation occur in distant and larger areas.

[51] As in the 2-D dynamic models presented above, the folding wavelength of Iberia is here related to the mechanical thickness of the plate. It is remarkable that the used elastic thickness derived independently for the Ebro Basin and Guadalquivir Basin successfully predict the range of observed wavelengths of folding of Iberia, thus revealing consistency between the flexural models of the northern and southern plate edge and the intraplate deformation model described here.

[52] In summary, transport along the river network contributes to enhance and localize vertical movements, and introduces lateral asymmetries in spatial patterns of erosion and sediment accumulation, as actually observed in Iberia. The study of paleoplanation surfaces has been often used to detect the presence of regional vertical movements potentially related to processes of crustal or lithospheric scale [e.g., *Bonnet et al.*, 2000; *Van Balen et al.*, 2000]. These types of studies may help significantly to further improve the understanding of present relief in Iberia.

8.4. Other Examples of Folding in Variscan Lithosphere

[53] An important factor in favor of the lithosphere folding scenario is a resemblance of the wavelength of deformation, thermotectonic age and the total amount of shortening to other known cases of continental lithospheric folding. A prominent example of folding can be found in the Western Goby area in central Asia with a thermotectonic age of 400 Ma. In this area, mantle and crustal wavelengths are 360 km and 50 km, respectively, with a shortening rate of $\sim$10 mm/yr and a total amount of shortening of 200–250 km during 10–15 Myr [*Burov et al.*, 1998; *Burov and Molnar*, 1998].

[54] Another case of recently detected folding in Variscan lithosphere is the Armorican Massif of Brittany at the western margin of the Paris Basin [*Bonnet et al.*, 1998, 2000]. The wavelength of the folds is 250 km, pointing to a lithospheric mantle control of the deformation. As pointed out by *Bonnet et al.* [2000], the spatial pattern and the timing of the uplift inferred from river incision studies of Brittany is incompatible with a glacio-eustatic origin. These

authors link the observed patterns of vertical motions in NW France to the present-day NW-SE oriented main axis of compression of the intraplate stress field of NW Europe. The stress-induced uplift pattern appears to control the amount of fluvial incision in the area as well as the location of the main drainage divides. The area located at the western margin of the Paris Basin and the Atlantic rifted margin of France has been subject to thermal rejuvenation during Mesozoic extension related to North Atlantic rifting and subsequent compressional intraplate deformation [*Ziegler et al.*, 1995], also affecting the Paris Basin [*Lefort and Agarwal*, 1996]. Leveling studies of the area [*LeNotre et al.*, 1999] also point to an ongoing deformation of the area.

[55] The inferred wavelengths for neotectonic lithosphere folds in Variscan lithosphere are consistent with the general relationships established between folding wavelength and thermotectonic age of the continental lithosphere, recognized in a number of folded areas of the globe [*Cloetingh and Burov*, 1996]. In Figure 12 we have plotted the wavelength of folding of Variscan lithosphere, inferred for Iberia and Brittany. In a number of other areas of continental lithosphere folding also smaller wavelength crustal folds have been detected, for example in central Asia [*Nikishin et al.*, 1993; *Cobbold et al.*, 1993]. This notion opens the perspective for a possible existence of a smaller, hitherto overlooked system of shorter wavelength upper crustal folds in Iberia.

9. Conclusions

[56] The following points summarize our conclusions.

1. The overall modeled patterns of lithosphere deformation are consistent with Alpine to recent reactivation of Hercynian lithosphere by development of compressional instabilities. It should be noted that because of slowly increasing growth rate, at low rates of shortening these instabilities take some time to develop important amplitudes (1 km). This time ranges from 5 to 10 Ma and depends on many factors such as rheology, structure, and geometry of the lithosphere and surface process activity.

It appears that partial coupling/decoupling between the crustal and mantle lithosphere may explain the existence of different wavelengths of deformation observed in Iberia. The modeling suggests that the observed short wavelengths ($\sim$50 km) can partly result from folding of the upper crustal brittle layer, and partly from distributed faulting controlled by the effective thickness of the brittle crustal layer (Figure 8b).

2. Models that include weakness zones in the southern margin of Iberia suggest that shortening from the south in itself is not capable to induce large-scale propagation of deformation over the whole Iberian lithosphere. Models subjected to symmetric shortening, however, produce very realistic deformation patterns, in particular reproducing lateral variation in deformation.

3. The modeling suggests that shortening from the north might be more important than previously thought, not only for the Early Tertiary but also for the Late Neogene evolution of Iberia. This is consistent with the preservation of the earlier (50 Ma) folding in the relatively cold (thermotectonic age of 350 Ma) northern part of Iberia until the onset of the new folding stage at 20 Ma associated with Betics compression from the south.

4. Erosion appears to be a largely overlooked factor in the discussion of the intraplate lithosphere deformation in Iberia. It plays a major role in the attenuation of the amplitude of the shorter (50 km) wavelength of surface topography. Erosion also accelerates vertical movements on the newly created and preexisting faulted structures (Figure 8b) in all bandwidths. In turn, the self-organization of the drainage network during folding determines the asymmetric surface mass redistribution.

[57] **Acknowledgments.** Contribution NSG20011201 of the Netherlands Research School of Sedimentary Geology. Funding through the PRIOR Project (CSN-ENRESA-IGN) to G. de Vicente and funding of E. Burov through the INSU IT program are gratefully acknowledged. We thank Marlies ter Voorde and Gerco Stapel for helpful discussions on an early version of the manuscript. We are thankful to both reviewers and to the associate editor for helpful and in-depth comments on the paper. The numerical code used in this paper is a modification of the Paravoz code, which kernel is developed by A. Poliakov and Y. Podladchikov, who are acknowledged for helpful and fruitful discussions.

References

Andeweg, B., Cenozoic tectonic evolution of the Iberian Peninsula, the effects and causes of changing stress fields, Ph.D. thesis, 178 pp., Vrije Univ., Amsterdam, 2002.

Andeweg, B., and S. Cloetingh, Evidence for an active sinistral shear zone in the Western Alboran region, *Terra Nova*, *13*, 44–50, 2001.

Andeweg, B., G. de Vicente, S. Cloetingh, J. Giner, and A. Muñoz Martin, Local stress fields and intraplate deformation of Iberia: Variations in spatial and temporal interplay of regional stress sources, *Tectonophysics*, *305*, 153–164, 1999.

Avouac, J.-P., and E. B. Burov, Erosion as a driving mechanism of intracontinental mountain growth, *J. Geophys. Res.*, *110*, 17,747–17,769, 1996.

Bada, G., S. Cloetingh, P. Gerner, and F. Horvath, Sources of recent tectonic stress in the Pannonian region: Inferences from finite element modelling, *Geophys. J. Int.*, *134*, 87–101, 1998.

Banda, E., Crustal parameters in the Iberian Peninsula, *Phys. Earth Planet. Int.*, *51*, 222–225, 1988.

Beaumont, C., P. Fullsack, and W. Hamilton, Erosional control of active compressional orogens, in *Thrust Tectonics*, edited by K. R. McClay, pp. 1–18, Chapman and Hall, New York, 1992.

Beekman, F., J. M. Bull, S. Cloetingh, R. A. Scrutton, Crustal fault reactivation facilitating lithospheric folding/buckling in the central Indian Ocean, *Geol. Soc. Spec. Publ., 99*, 251–263, 1996.

Ben-Avraham, Z., and A. Ginzburg, Displaced terranes and crustal evolution of the Levant and the eastern Mediterranean, *Tectonics*, *9*, 613–622, 1990.

Blanco, M.-J., and W. Spakman, The P-wave velocity structure of the mantle below the Iberian Peninsula: Evidence for subducted lithosphere below southern Spain, *Tectonophysics*, *221*, 13–34, 1993.

Bonnet, S., F. Guillocheau, and J.-P. Brun, Relative uplift measured using river incision: The case of the Armorican basement (France), *C. R. Acad. Sci. Paris, Ser. II*, *327*, 245–251, 1998.

Bonnet, S., F. Guillocheau, J.-P. Brun, and J. Van den Driessche, Large-scale relief development related to Quaternary tectonic uplift of a Proterozoic-Paleozoic basement: The Armorican Massif, NW France, *J. Geophys. Res.*, *105*, 19,273–19,288, 2000.

Borges, J. F., A. J. S. Fitas, M. Bezzeghoud, and P. Teves-Costa, Seismotectonics of Portugal and its adjacent Atlantic area, *Tectonophysics*, *337*, 373–387, 2001.

Brace, W. F., and D. L. Kohlstedt, Limits on lithospheric stress imposed by laboratory experiments, *J. Geophys. Res.*, *85*, 6248–6252, 1980.

Braun, J., and M. Sambridge, Modelling landscape evolution on geological time scales: A new method based on irregular spatial discretization, *Basin Res.*, *9*, 27–52, 1997.

Burov, E. B., and S. Cloetingh, Erosion and rift dy-

namics: New thermomechanical aspects of post-rift evolution of extensional basins, *Earth Planet Sci. Lett.*, *150*, 7–26, 1997.

Burov, E. B., and M. Diament, The effective elastic thickness (T_e) of continental lithosphere: What does it really mean?, *J. Geophys. Res.*, *100*, 3905–3927, 1995.

Burov, E. B., and L. Guillou-Frottier, Thermomechanical behavior of large ash flow calderas, *J. Geophys. Res.*, *104*, 23,081–23,109, 1999.

Burov, E. B., and P. Molnar, Gravity anomalies over the Ferghana Valley (central Asia) and intracontinental deformation, *J. Geophys. Res.*, *103*, 18,137–18,152, 1998.

Burov, E. B., and A. N. B. Poliakov, Erosion and rheology controls on synrift and postrift evolution: Verifying old and new ideas using a fully coupled numerical model, *J. Geophys. Res.*, *106*, 16,461–16,481, 2001.

Burov, E. B., L. I. Lobkovsky, S. Cloetingh, and A. M. Nikishin, Continental lithosphere folding in Central Asia (part II): Constraints from gravity and topography, *Tectonophysics*, *226*, 73–88, 1993.

Burov, E. B., J.-C. Marechal, and C. Jaupart, Large-scale crustal inhomogeneities and lithospheric strength in cratons, *Earth Planet Sci. Lett*, *164*, 205–219, 1998.

Caporali, A., Buckling of the lithosphere in western Himalaya: Constraints from gravity and topography data, *J. Geophys. Res.*, *105*, 3103–3113, 2000.

Carter, N. L., and M. C. Tsenn, Flow properties of continental lithosphere, *Tectonophysics*, *136*, 27–63, 1987.

Casas, A., and R. Salas, Mesozoic extensional stratigraphy and crustal evolution during the Alpine cycle of the East Iberian basin, *Tectonophysics*, *228*, 33–56, 1993.

Casas-Sainz, A. M., A. L. Cortés-Gracia, and A. Maestro-Gonzáles, Intraplate deformation and basin formation during the Tertiary within the northern Iberian plate: Origin and evolution of the Almazán Basin, *Tectonics*, *19*, 258–289, 2000.

Castellote, M., and CuaTeNeo team, CuaTeNeo GPS network to monitor crustal deformation in the SE of the Iberian Peninsula, paper presented at the Tenth General Assembly of the WEGENER Project (WEGENER 2000), R. Inst. and Obs. of the Army, Minist. of Def., Spain, San Fernando, Spain, Sep. 18–20, 2000.

Cloetingh, S., Intraplate stress: New element in basin analysis, in *New Perspectives in Basin Analysis*, edited by K. L. Kleinspehn and C. Paola, pp. 205–230, Springer-Verlag, New York, 1988.

Cloetingh, S., and E. B. Burov, Thermomechanical structure of European continental lithosphere: Constraints from rheological profiles and EET estimates, *Geophys. J. Int.*, *127*, 399–414, 1996.

Cloetingh, S., and M. J. R. Wortel, Regional stress field of the Indian plate, *Geophys. Res. Lett.*, *12*, 77–80, 1985.

Cloetingh, S., H. McQueen, and K. Lambeck, On a tectonic mechanism for relative sea level fluctuations, *Earth Planet. Sci. Lett.*, *75*, 157–166, 1985.

Cloetingh, S., P. A. Van der Beek, D. Van Rees, T. B. Roep, C. Biermann, and R. A. Stephenson, Flexural interaction and the dynamics of Neogene extensional basin formation in the Alboran-Betic region, *Geo. Mar. Lett.*, *12*, 66–75, 1992.

Cloetingh, S., E. Burov, and A. Poliakov, Lithosphere folding: Primary response to compression? (from central Asia to Paris basin), *Tectonics*, *18*, 1064–1083, 1999.

Cobbold, P., P. Davy, D. Gapais, E. A. Rossello, E. Sadybakasov, J. C. Thomas, J. J. Tondji Biyo, and M. de Urreiztieta, Sedimentary basins and crustal shortening, *Sediment. Geol.*, *86*, 77–89, 1993.

Cundall, P. A., Numerical experiments on localization in frictional materials, *Ing. Arch.*, *59*, 148–159, 1989.

De Bruijne, C. H., and P. A. M. Andriessen, Interplay of intraplate tectonics and surface processes in the Sierra de Guadarrama (central Spain), assessed by apatite fission track analysis, *Phys. Chem. Earth, Part A*, *25*, 555–563, 2000.

De Bruijne, C. H., and P. A. M. Andriessen, Fault related denudation in the Spanish Central System (central Spain), recording the far field effects of Alpine plate tectonic history of the Iberian microplate, *Tectonophysics*, *349*, 161–184, 2002.

De Jong, K., J. R. Wijbrans, and G. Feraud, Repeated thermal resetting of phengites during Miocene extension and wrenching in the Betic Cordilleras, SE Spain●Evidence from $^{40}AR/^{39}AR$ step-heating and single grain argon laser probe dating in the Mulhacen Complex, *Earth Planet. Sci. Lett.*, *110*, 173–191, 1992.

DeMets, C., R. G. Gordon, D. F. Argus, and S. Stein, Effect of revisions to geomagnetic reversal time scale on estimated current plate motions, *Geophys. Res. Lett.*, *21*, 2191–2194, 1994.

de Vicente, G., J. L. Giner, A. Muñoz Martin, J. M. Gonzalez-Casado, and R. Lindo, Determination of present-day stress tensor and neotectonic interval in the Spanish Central System and Madrid Basin, central Spain, *Tectonophysics*, *266*, 405–424, 1996.

Dewey, J. F., M. L. Helman, E. Turco, D. H. W. Hutton, and S. D. Knott, Kinematics of the western Mediterranean, in *Alpine Tectonics*, edited by M. P. Coward, D. Dietrich, and D. G. Park, *Geol. Soc. Spec. Publ., 45*, 265–283, 1989.

Docherty, C., and E. Banda, Evidence for the eastward migration of the Alboran Sea based on regional subsidence analysis: A case for basin delamination of the subcrustal lithosphere?, *Tectonics*, *14*, 804–814, 1995.

Faccenna, C., F. Funiciello, D. Giardini, and P. Lucente, Episodic back-arc extension during restricted mantle convection in the Central Mediterranean, *Earth Planet. Sci. Lett.*, *187*, 105–116, 2001.

Fernandes, R., B. Ambrosius, R. Noomen, L. Basos, and J. Davila, Analysis of a permanent GPS Iberian network (GIN), paper presented at the 10th General Assembly of the Wegener Project (WEGENER 2000), R. Inst. and Obs. of the Army, Minist. of Def., Spain, San Fernando, Spain, Sep. 18–20, 2000.

Fernandez, M., I. Marzan, A. Lorreia, and E. Ramalho, Heat flow, heat production and lithospheric thermal regime in the Iberian Peninsula, *Tectonophysics*, *291*, 29–53, 1998.

Fitzgerald, P. G., J. A. Munoz, P. J. Coney, and S. L. Baldwin, Asymmetric exhumation across the Pyrenean orogen: Implications for the tectonic evolution of a collisional orogen, *Earth Planet. Sci. Lett.*, *173*, 157–170, 1999.

Friend, P. F., and C. J. Dabrio, *Tertiary Basins of Spain*: *The Stratigraphic Record of Crustal Kinematics*, *World Reg. Geol. Ser.*, vol. 6, edited by P. F. Friend and C. J. Dabrio, 412 pp., Cambridge Univ. Press, New York, 1996.

Gallagher, K., Evolving temperature histories from apatite fission track data, *Earth Planet. Sci. Lett.*, *136*, 421–435, 1995.

Garcia-Castellanos, D., Lithospheric control of drainage in foreland basins, *Basin Res.*, *14*, 89–104, 2002.

Garcia-Castellanos, D., M. Fernàndez, and M. Torne, Modeling the evolution of the Guadalquivir foreland basin (southern Spain), *Tectonics*, *21*(3), 1018, doi:10.1029/2001TC001339, 2002.

Gaspar-Escribano, J. M., J. D. van Wees, M. ter Voorde, S. Cloetingh, E. Roca, L. Cabrera, J. A. Muñoz, P. A. Ziegler, and D. García-Castellanos, 3D flexural modeling of the Ebro Basin (NE Iberia), *Geophys. J. Int.*, *145*, 349–368, 2001.

Gerbault, M., E. B. Burov, A. Poliakov, and M. Daignieres, Do faults trigger folding in the lithosphere?, *Geophys. Res. Lett.*, *26*, 271–274, 1999.

Golke, M., and D. Coblentz, Origins of the European regional stress field, *Tectonophysics*, *266*, 11–24, 1996.

Gonzales, A., D. Cordoba, R. Vegas, and L. M. Matias, Seismic crustal structure in the southwest of the Iberian Peninsula and the Gulf of Cadiz, *Tectonophysics*, *296*, 317–331, 1998.

Guillocheau, F., Meso-Cenozoic geodynamic evolution of the Paris Basin: 3D stratigraphic constraints, *Geodyn. Acta*, in press, 2002.

Herraiz, M., G. de Vicente, R. Lindo, and J. G. Sanchez-Cabanero, Seismotectonics of the Sierra Albarrana area (southern Spain): Constraints for a regional model of the Sierra Morena-Guadalquivir Basin limit, *Tectonophysics*, *266*, 425–442, 1996.

Howard, A. D., W. E. Dietrich, and M. A. Seidl, Modeling fluvial erosion on regional to continental scales, *J. Geophys. Res.*, *99*, 13,971–13,986, 1994.

Hunt, G., H. Muhlhaus, B. Hobbs, and A. Ord, Localized folding of viscoelastic layers, *Geol. Rundsch.*, *85*, 58–64, 1996.

Janssen, M. E., M. Torne, S. Cloetingh, and E. Banda, Pliocene uplift of the eastern Iberian margin: Inferences from quantitative modeling of the Valencia Trough, *Earth Planet. Sci. Lett.*, *119*, 585–597, 1993.

Juez Larre, J., and P. A. M. Andriessen, Post Late Paleozoic tectonism in the southern Catalan Coastal Ranges (NE Spain), assessed by apatite fission track analysis, *Tectonophysics*, *349*, 113–129, 2002.

Jurado, M. J., and B. Mueller, Contemporary tectonic stress in NE Iberia: New evidence from borehole break-out analysis, *Tectonophysics*, *282*, 99–115, 1997.

Kirby, S. H., and A. K. Kronenberg, Rheology of the lithosphere: Selected topics, *Rev. Geophys.*, *25*, 1219–1244, 1987.

Kooi, H., and C. Beaumont, Escarpment retreat on high-elevation rifted continental margins: Insights derived from a surface process model that combines diffusion, reaction, and advection, *J. Geophys. Res.*, *99*, 12,191–12,202, 1994.

Kooi, H., and C. Beaumont, Large-scale geomorphology: Classical concepts reconciled and integrated with contemporary ideas via a surface process model, *J. Geophys. Res.*, *101*, 3361–3386, 1996.

Lambeck, K., The role of compressive forces in intracratonic basin formation and mid-plate orogenies, *Geophys. Res. Lett.*, *10*, 845–848, 1983.

Lefort, J. P., and P. Agarwal, Gravity evidence for an Alpine buckling of the crust beneath the Paris Basin, *Tectonophysics*, *258*, 1–14, 1996.

Lenotre, N., P. Thierry, R. Blanchin, and G. Brochard, Current vertical movement demonstrated by comparative leveling in Brittany (France), *Tectonophysics*, *301*, 333–344, 1999.

Marshak, S., B. A. Van der Pluim, and M. Hamburger, The tectonics of continental interiors (preface), in *The Tectonics of Continental Interiors*, edited by S. Marshak, B. A. Van der Pluim, and M. Hamburger, *Tectonophysics, 305*, vii–x, 1999.

Martinod, J., and P. Davy, Periodic instabilities during compression of the lithosphere, 2, Analogue experiments, *J. Geophys. Res.*, *99*, 57–69, 1994.

Masson, D. G., J. A. Cartwright, L. M. Pinheiro, R. B. Whitmarsh, M.-O. Beslier, and H. Roeser, Compressional deformation at the continent-ocean transition in the NE Atlantic, *J. Geol. Soc. London*, *15*, 607–613, 1994.

Mezcua, J., A. Gil, and R. Benarroch, Estudio gravimetrico de la Peninsula Iberica y Baleares, *Inst. Geogr. Nac.*, 19 pp., 2 sheets, 1996.

Millan, H., B. T. den Bezemer, J. Verges, M. Marzo, J. A. Munoz, E. Roca, J. Cires, R. Zoetemeijer, S. Cloetingh, and C. Puigdefabregas, Paleo-elevation and EET evolution of mountain ranges: Inferences from flexural modeling in the Eastern Pyrenees and Ebro Basin, *Mar. Pet. Geol.*, *12*, 917–928, 1995.

Munoz, J. A., Evolution of a continental collision belt: ECORS-Pyrenees crustal balanced cross-section, in *Thrust Tectonics*, edited by K. McClay, pp. 235–246, Chapman and Hall, New York, 1992.

Nikishin, A. M., S. Cloetingh, L. Lobkovsky, and E. B. Burov, Continental lithosphere folding in central Asia, part I, Constraints from geological observations, *Tectonophysics*, *226*, 59–72, 1993.

Ordonez Casado, B., D. Gebauer, H. J. Schafer, J. I. G. Ibarguchi, and J. J. Peucat, A single Devonian subduction event for the HP/HT metamorphism of the

Cabo Ortegal complex within the Iberian Massif, *Tectonophysics*, *332*, 359–385, 2001.

Peper, T., and S. Cloetingh, Lithosphere dynamics and tectono-stratigraphic evolution of the Mesozoic Iberian rifted margin (southeastern Spain), *Tectonophysics*, *203*, 345–361, 1992.

Poliakov, A. N. B., Y. Podladchikov, and C. Talbot, Initiation of salt diapirs with frictional overburden: Numerical experiments, *Tectonophysics*, *228*, 199–210, 1993.

Ribeiro, A., M. C. Kullberg, J. C. Kullberg, G. Manuppella, and S. Phipps, A review of Alpine tectonics in Portugal: Foreland detachment in basement and cover rocks, *Tectonophysics*, *184*, 357–366, 1990.

Ribeiro, A., J. Cabral, R. Baptista, and L. Matias, Stress pattern in Portugal mainland and the adjacent Atlantic region, West Iberia, *Tectonics*, *15*, 641–659, 1996.

Richardson, R. M., S. C. Solomon, and N. H. Sleep, Tectonic stress in the plates, *Rev. Geophys.*, *17*, 981–1019, 1979.

Roest, W. R., and S. P. Srivastava, Kinematics of the plate boundaries between Eurasia, Iberia, and Africa in the North Atlantic from the late Cretaceous to the present, *Geology*, *19*, 613–616, 1991.

Rutigliano, P., and VLBI Network team, Vertical motions in the western Mediterranean area from geodetic and geological data, paper presented at the Tenth General Assembly of the WEGENER Project (WEGENER 2000), R. Inst. and Obs. of the Army, Minist. of Def., Spain, San Fernando, Spain, Sep. 18–20, 2000.

Seber, D., M. Barazangi, A. Ibenbrahim, and A. Demnati, Geophysical evidence for lithospheric delamination beneath the Alboran Sea and Rif-Betic mountains, *Nature*, *379*, 785–790, 1996.

SIGMA, Proyecto SIGMA, Análisis del estado de esfuerzos tectónicos, reciente y actual en la Península Ibérica, in *Colección Otros Documentos*, vol. 10, 239 pp., Consejo de Seguridad Nuclear, Madrid, 1998.

Simancas, J. F., D. Martinez Poyatos, I. Exposito, A. Azor, and F. Gonzales Lodeiro, The structure of a major suture zone in the SW Iberian Massif: The Ossa-Morena/Central Iberian contact, *Tectonophysics*, *332*, 295–308, 2001.

Stapel, G., The nature of isostasy in western Iberia, Ph.D. thesis, 148 pp., Vrije Univ., Amsterdam, 1999.

Stapel, G., S. Cloetingh, and B. Pronk, Quantitative subsidence analysis of the Mesozoic evolution of the Lusitanian Basin (Western Iberian margin), *Tectonophysics*, *266*, 493–507, 1996.

Stephenson, R. A., and S. Cloetingh, Some examples and mechanical aspects of continental lithospheric folding, *Tectonophysics*, *188*, 27–37, 1991.

Tsenn, M. C., and N. L. Carter, Flow properties of continental lithosphere, *Tectonophysics*, *136*, 27–63, 1987.

Tucker, G. E., and R. Slingerland, Controls on sediment flux from fold and thrust belts, results from models based on the Zagros Orogen, *Geol. Soc. Am Abst. Programs*, *27*(6), 380, 1995.

Turcotte, D., and G. Schubert, *Geodynamics, Applications of Continuum Physics to Geological Problems*, John Wiley, New York, 1982.

Van Balen, R. T., R. F. Houtgast, F. M. Van der Wateren, J. Vandenberghe, and P. W. Bogaart, Sediment budget and tectonic evolution of the Meuse catchment in the Ardennes and the Roer Valley Rift System, *Global Planet. Change*, *27*, 113–129, 2000.

Van der Beek, P. A., and J. Braun, Numerical modelling of landscape evolution on geological time-scales: A parameter analysis and comparison with the south-eastern highlands of Australia, *Basin Res.*, *10*, 49–68, 1998.

Van der Beek, P. A., and S. Cloetingh, Lithospheric flexure and the tectonic evolution of the Betic cordilleras, *Tectonophysics*, *203*, 325–344, 1992.

Van der Pluim, B. A., J. P. Craddock, B. R. Graham, and J. H. Harris, Paleostress in cratonic North America: Implications for deformation of continental interiors, *Science*, *277*, 794–796, 1997.

Van Wees, J. D., and S. Cloetingh, A finite-difference technique to incorporate spatial variations in rigidity and planar faults into 3-D models for lithospheric flexure, *Geophys. J. Int.*, *117*, 179–195, 1994.

Van Wees, J. D., K. de Jong, and S. Cloetingh, Two-dimensional P-T-t modeling and the dynamics of extension and compression in the Betic Zone, *Tectonophysics*, *203*, 305–324, 1992.

Van Wees, J. D., S. Cloetingh, and G. de Vicente, The role of preexisting faults in basin evolution: Constraints from 2D finite element and 3D flexure models, in *Modern Developments in Structural Interpretation, Validation and Modelling*, edited by P. G. Buchanan and D. A. Nieuwland, *Geol. Soc. Spec. Publ., 99*, 297–320, 1996.

Van Wees, J. D., A. Arche, C. G. Beijdorff, J. Lopez-Gomez, and S. A. P. L. Cloetingh, Temporal and spatial variations in tectonic subsidence in the Iberian Basin (eastern Spain): Inferences from automated modelling of high-resolution stratigraphy (Permian-Mesozoic), *Tectonophysics*, *300*, 285–310, 1998.

Vegas, R., and E. Banda, Tectonic framework and Alpine evolution of the Iberian Peninsula, *Earth Evol. Sci.*, *4*, 320–343, 1982.

Vegas, R., J. T. Vazquez, E. Surinach, and A. Marcos, Model of distributed deformation, block rotation and crustal thickening for the formation of the Spanish Central System, *Tectonophysics*, *184*, 367–378, 1990.

Verges, J., M. Marzo, T. Santaeularia, J. Serra-Kiel, D. W. Burbank, J. A. Munoz, and J. Gimenez-Montsant, Quantified vertical motions and tectonic evolution of the SE Pyrenean foreland basin, *Geol. Soc. Spec. Publ., 134*, 107–134, 1998.

Waltham, D., C. Docherty, and C. Taberner, Decoupled flexure in the South Pyrenean foreland, *J. Geophys. Res.*, *105*, 16,329–16,339, 2000.

Whipple, K. X., and G. E. Tucker, Dynamics of the stream-power river incision model: Implications for height limits of mountain ranges, landscape response timescales, and research needs, *J. of Geophys. Res.*, *104*, 17,661–17,674, 1999.

Willgose, G., R. J. Bras, and I. I. Rodriges, Results from a new model of river basin evolution, *Earth Surf. Processes Landforms*, *16*, 237–254, 1991.

Wortel, R., and W. Spakman, Subduction and slab detachment in the Mediterranean-Carpathian region, *Science*, *290*, 1910–1917, 2000.

Zeck, H. P., P. Monie, I. M. Villa, and B. T. Hansen, Very high rates of cooling and uplift in the Alpine belt of the Betic Cordilleras, southern Spain, *Geology*, *20*, 79–82, 1992.

Ziegler, P. A., S. Cloetingh, and J. D. Van Wees, Geodynamics of intraplate compressional basin deformation: The Alpine foreland and other examples, *Tectonophysics*, *252*, 7–59, 1995.

Ziegler, P. A., J. D. Van Wees, and S. Cloetingh, Mechanical controls on collision related compressional intraplate deformation, *Tectonophysics*, *300*, 103–129, 1998.

Ziegler, P. A., G. Bertotti, and S. Cloetingh, Dynamic processes controlling foreland development•The role of mechanical (de)coupling of orogenic wedges and forelands, *EGS Spec. Publ.*, *1*, 29–91, 2002.

Zoback, M. L., First- and second-order patterns of stress in the lithosphere: The World Stress Map project, *J. Geophys. Res.*, *97*, 11,703–11,728, 1992.

B. Andeweg, P. A. M. Andriessen, F. Beekman, S. Cloetingh, and D. Garcia-Castellanos, Netherlands Research Centre for Integrated Solid Earth Science, Faculty of Earth and Life Sciences, Vrije Universiteit, De Boelelaan 1085, NL-1081 HV Amsterdam, Netherlands. (andb@geo.vu.nl; andp@geo.vu.nl; beef@geo.vu.nl; cloeting@geo.vu.nl; gard@geo.vu.nl)

E. Burov, Laboratoire de Tectonique, UMR 7072, University of P. et M. Curie, 4 Place Jussieu, F-75252 Paris Cedex 05, France. (evgenii.burov@lgs.jussieu.fr)

R. Vegas and G. de Vicente, Faculty of Geological Sciences, Universidad Complutense de Madrid, E-28040 Madrid, Spain. (ruidera@eucmax.sim.ucm.es; smartin@geo.ucm.es)